1 **Laboratory Assessment of the Impact of Chemical Oxidation, Mineral**

2 **Dissolution, and Heating on the Nitrogen Isotopic Composition of Fossil-**

3 **bound Organic Matter**

4
5

6 **Alfredo Martínez-García*[1], Jonathan Jung[1], Xuyuan E. Ai[1,2], Daniel M. Sigman[2],**

7 **Alexandra Auderset[1], Nicolas Duprey[1], Alan Foreman[1], François Fripiat[1,3], Jennifer**

8 **Leichliter[1], Tina Lüdecke [1], Simone Moretti[1], Tanja Wald[1]**

9

10 *[1] Max Planck Institute for Chemistry, Mainz, Germany*

11 *[2] Princeton University, Princeton, USA*

12 *[3] Université Libre de Bruxelles, Brussels, Belgium*

13

14 *corresponding author: Alfredo Martínez-García (a.martinez-garcia@mpic.de)

15

16

17

18 **Key Points:**
19
20 - Fossil-bound organic matter is well protected from chemical changes in the
21 surrounding environment by the mineral matrix.

22 - Partial dissolution of fossil calcite, aragonite, opal, and enamel has a negligible effect
23 on their N isotopic composition and N content.

24 - During heating, fossil N content and isotopic composition remains unchanged if the
25 structure of the inorganic matrix is not compromised.

26

27

28   **Abstract**

29   Fossil-bound organic material holds great potential for the reconstruction of past changes in

30   nitrogen (N) cycling. Here, with a series of laboratory experiments, we assess the potential effect

31   of oxidative degradation, fossil dissolution, and thermal alteration on the fossil-bound N isotopic

32   composition of a range of fossil types, including deep and shallow water scleractinian corals,

33   foraminifera, diatoms and tooth enamel. Our experiments show that exposure to different

34   strongly oxidizing reagents does not significantly affect the N isotopic composition or N content

35   of any of the fossil types analyzed, demonstrating that organic matter is well protected from

36   changes in the surrounding environment by the mineral matrix. In addition, we show that partial

37   dissolution (up to 70-90%) of fossil aragonite, calcite, opal, or enamel matrixes has a negligible

38   effect on the N isotopic composition or N content of the fossils. These results suggest that the

39   isotopic composition of fossil-bound organic material is relatively uniform, and also that N

40   exposed during dissolution is lost without significant isotopic discrimination. Finally, our heating

41   experiments show negligible changes in the N isotopic composition and N content of all fossil

42   types at 100 ℃. At 200 ℃ and hotter, the N loss and associated nitrogen isotope changes appear

43   to be directly linked to the sensitivity of the mineral matrix to thermal stress. These results

44   suggest that, so long as high temperature does not compromise the mineral structure, the

45   biomineral matrix acts as a closed system with respect to N, and the N isotopic composition of

46   the fossil remains unchanged.

47

48   **Plain Language Summary**

49   The ratio of the heavy and light isotopes of nitrogen (^{15}N and ^{14}N) in the organic material

50   contained within the mineral structure of fossils can be used to reconstruct past changes in

51   biological and chemical processes. With a series of laboratory experiments, we evaluate the

52   potential effects of chemical conditions, fossil dissolution, and heating on the nitrogen isotopic

53   composition (^{15}N/^{14}N ratio) of corals, foraminifera, diatoms and teeth. Our results indicate that

54   these processes do not have a significant effect on the ^{15}N/^{14}N of fossils, suggesting that the

55   mineral matrix provides a barrier that isolates a fossil's organic nitrogen from the surrounding

56   environment, preventing alteration of its ^{15}N/^{14}N. In addition, we show that if part of the fossil-

57   bound organic nitrogen is exposed by dissolution or heating, it is lost without affecting the

58   ^{15}N/^{14}N of the organic material that remains in the mineral. These findings imply that the original

59    $^{15}N/^{14}N$ ratio incorporated by the organism is preserved in the geologic record. Therefore,

60   measurements of the nitrogen isotopes on fossils can provide faithful ecological and

61   environmental information about the past.

62   **1 Introduction**

63   The stable isotopes of nitrogen (^{14}N and ^{15}N) can offer important insights into present and past

64   changes in the cycling of this key element through organisms, food webs, and environments

65   (Casciotti, 2016; Deniro and Epstein, 1981; Fripiat et al., 2021; Sigman and Fripiat, 2019; Straub

66   et al., 2021; Wolf et al., 2009). Their use in paleo-reconstructions requires the development of

67   faithful geochemical archives that are unaffected by diagenetic alteration and/or contamination

68   by exogenous N. In recent years, the analysis of the N isotopic composition of the organic matter

69   bound within the mineral structure of fossil skeletons (e.g., foraminifera, corals, diatoms, otoliths

70   and tooth enamel) has emerged as a promising archive of the original isotopic signature of the

71   organism that is protected from degradation for thousands to millions of years (Ai et al., 2020;

72   Altabet and Curry, 1989; Duprey et al., 2020; Erler et al., 2020; Erler et al., 2016; Farmer et al.,

73   2021; Kast et al., 2019; Leichliter et al., 2021; Lueders-Dumont et al., 2018; Martinez-Garcia et

74   al., 2014; Ren et al., 2017; Ren et al., 2009; Robinson et al., 2004; Robinson et al., 2005;

75   Shemesh et al., 1993; Sigman et al., 1999; Sigman et al., 2021; Straub et al., 2013; Studer et al.,

76   2021; Studer et al., 2015; Studer et al., 2018; Wang et al., 2014; Wang et al., 2016; Wang et al.,

77   2017).

78

79   The compounds that comprise fossil-bound organic matter play an active, but still poorly

80   understood, physiological role in the biomineralization process. In planktonic foraminifera and

81   stony corals, this organic matter consists of a series of proteins and polysaccharides that regulate

82   the calcification process (Weiner and Erez, 1984), with recent suggestions of a lipid component

83   as well (Swart et al., 2021). In enamel, a series of specific proteins (amelogenin, enamelin,

84   amelotin, and ameloblastin) play a key role as the structural scaffolds that determine mineral

85   morphology during enamel development (Bai et al., 2020; Castiblanco et al., 2015). Although

86   most of these organic compounds are digested and removed at the enamel maturation stage to

87   achieve maximum hardness, these specific proteins are still found in tooth enamel samples that

88   are millions of years old (Cappellini et al., 2019). In diatoms, frustule-bound organic matter is

89   composed mainly of a set of taxon-specific polyamines and silaffins that promote silica

90   precipitation during the formation of the diatom frustule (Bridoux et al., 2012a; Bridoux et al.,

91   2012b; Kroger, 2002; Kroger et al., 2000). Fossil-bound organic material is, therefore, native to

92   the organism.

93

94   Several lines of evidence suggest that the mineral matrix provides an effective barrier that

95   protects the native, fossil-bound organic matter from contamination by external organic material

96   from the surrounding sedimentary environment. For example, the amino acid composition of

97   fossil-bound organic matter has significant differences from cooccurring organic matter in the

98   sedimentary environment. The non-proteinogenic amino acids β-alanine and γ-aminobutyric are

99   formed by microbial decarboxylation of aspartic and glutamic acids, making them ubiquitously

100   abundant in marine sediments (Cowie and Hedges, 1994; Dauwe and Middelburg, 1998;

101   Whelan, 1977). Thus, the absence of these amino acids in foraminifera tests suggests that the

102   mineral matrix provides an effective barrier against microbial attack of fossil-bound organic

103   matter and prevents the exchange of compounds with the surrounding sediments (Schroeder,

104   1975). In addition, laboratory studies indicate that the racemization reaction proceeds without

105   significant impact on the nitrogen and carbon isotopic composition of the L- and D-enantiomers,

106   so that the isotopic comparison of the enantiomers can be used to assess contamination of fossil-

107   bound organic material (Engel and Macko, 1986). For example, the similarity of the carbon

108   isotopic compositions of the D and L enantiomers of several individual amino acids in late

109   Pleistocene land snail shells confirmed that their shell-bound amino acids were indigenous to the

110   fossil (Engel et al., 1994). Finally, new biochemical and molecular biological tools are beginning

111   to be applied to fossil-bound organic matter and speak to its fossil-native origin. For example, a

112   recent analysis of the enamel proteome from a 1.77 Ma extinct Rhinoceros tooth has shown that

113   it is endogenous and almost complete (Cappellini et al., 2019).

114

115   The issue of endogeneity aside, there is also the possibility of effects of oxidative attack, mineral

116   dissolution, and thermal alteration on the N isotopic composition of fossil-bound organic

117   material. A key postulate in the application of the fossil-bound N isotope method is that the

118   mineral matrix provides an effective physical barrier that isolates organic compounds from the

119   surrounding environment, protecting them from both external contamination and chemical or

120   biological attack. The relative stability of the N content per mg of mineral of different fossil

121 types (e.g., planktonic foraminifera, diatoms, scleractinian corals and tooth enamel) over
122 thousands and even millions of years provides support for this postulate (Kast et al., 2019;
123 Leichliter et al., 2021; Ren et al., 2017; Studer et al., 2012; Wang et al., 2017). However, the
124 stability of the N isotopic composition in response to changes in external chemical conditions
125 that could favor organic matter degradation has not been systematically assessed.

126

127 Partial dissolution of the fossil mineral structure can have severe impacts on many geochemical
128 proxies that rely on the isotopic and/or elemental composition of the inorganic biomineral
129 matrix. These effects are thought to derive largely from the preferential dissolution of parts of the
130 biomineral that have a distinct elemental/isotopic composition (Brown and Elderfield, 1996;
131 McCorkle et al., 1995; Pearson, 2017; Rosenthal et al., 2000; Smith et al., 2016). In contrast,
132 dissolution is thought to have a minimal effect on the N isotopic composition of organic matter
133 bound within the biomineral structure of the fossils because: (i) the organic matter exposed after
134 dissolution should ultimately be degraded and/or removed during cleaning prior to analysis (see
135 section 2.2), and (ii) no reason is known for the isotopic composition of fossil-bound organic
136 matter to vary coherently with dissolution susceptibility across the biomineral structure.
137 However, so far, these two arguments have not been tested.

138

139 In addition, sedimentary organic matter degradation can increase during burial as a consequence
140 of the temperature rise associated with local geothermal gradients, potentially causing important
141 impacts on its molecular and isotopic composition (Burdige, 2006). Although typical thermal
142 gradients in Cenozoic marine sediments are relatively small (< 60 ºC) (Malinverno and Martinez,
143 2015), they can be substantially larger (> 500 ºC) in other depositional settings that contain
144 identifiable fossils (Rejebian et al., 1987). In any case, the potential effect of thermal degradation
145 on the nitrogen isotopic composition of fossil-bound organic matter has not been examined.

146

147 In this study, we report results from laboratory experiments designed to evaluate the potential
148 effects of oxidizing conditions, mineral dissolution, and thermal alteration on the nitrogen
149 isotopic composition of fossil-bound organic matter.

150

2 Materials and Methods

2.1 Sample Materials

The different experiments were performed using a series of sample materials prepared at the Max Plank Institute for Chemistry (MPIC) in Mainz, Germany. These materials are intended to be representative of different fossil types typically used in paleo-reconstructions (Table 1) and include: modern deep-sea (*Lophelia pertusa, LO-1*) and shallow water (*Porites sp., PO-1*) coral samples; late Holocene mixed foraminifera fractions (63-315 μm) from sediment cores collected in the North Atlantic (MF-1) and the Southern Ocean (MF-2); modern tooth enamel from an African elephant (*Loxodonta africana,* AG-Lox); fossil enamel from a Pleistocene (ca. 2.5 to 2.3 Ma) suid (*Notochoerus scotti*, Noto-2) from Zone 3A-2 of the Chiwondo Beds in Malawi (prepared from the same tooth as "Noto-1" reported in Leichliter et al. (2021)); fossil enamel from a Plio-Pleistocene (ca. 3.75 to 1.8 Ma) hippopotamus (*Hippopotamus amphibious,* Hippo-1) from Unit 3 at the Chiwondo Beds in Malawi; and two diatom samples obtained from sediment cores from the Antarctic Zone of the Southern Ocean (DI-1 and DI-2) prepared following the diatom separation methods described in (Studer et al., 2015) .

Table 1. Description of the sample materials analyzed in this study

MPIC-ID	Description/Genus/Species	Matrix	Location	Age	Reference
MF-1	Mixed Foraminifera, 63-315 μm size fraction	Calcite	North Atlantic	Late Holocene	*This study*
MF-2	Mixed Foraminifera, 63-315 μm size fraction	Calcite	Southern Ocean	Late Holocene	*This study*
PO-1	*Porites sp.*	Aragonite	Chuuk, Micronesia	Modern	*(Leichliter et al., 2021)*
LO-1	*Lophelia pertusa*	Aragonite	North Atlantic	Modern	*(Leichliter et al., 2021)*
AG-Lox	*Loxodonta africana*	Enamel	Africa	Modern	*(Gehler et al., 2012; Leichliter et al., 2021)*
Noto-2	*Notochoerus scotti*	Enamel	Malawi, Africa	2.3 - 2.5 Ma	*(Kullmer, 2008; Leichliter et al., 2021)*
Hippo-1	*Hippopotamus amphibius*	Enamel	Malawi, Africa	1.8- 3.75 Ma	*This study*
DI-1	Diatoms, < 63um size fraction	Opal	Southern Ocean, core PS75/72-2	MIS11 (374-424 ka)	*This study*
DI-2	Diatoms, < 63um size fraction	Opal	Southern Ocean, core PS69/899-2	MIS 5 (120-124 ka)	*This study*

2.2 Analysis of fossil-bound nitrogen isotopes

The analyses were performed in the laboratories of the Organic Isotope Geochemistry Group of the Department of Climate Geochemistry at the MPIC. The nitrogen isotopic composition (expressed as $\delta^{15}N = ((^{15}N/^{14}N)_{sample}/(^{15}N/^{14}N)_{air} - 1) *1000$) of the samples was determined using the oxidation-denitrifier method (Knapp et al., 2005). Prior to analysis, sample powders were chemically cleaned following standard reductive and oxidative cleaning steps that have been described previously for each fossil type (Leichliter et al., 2021; Ren et al., 2009; Studer et al., 2015; Wang et al., 2014), as described below.

The reductive cleaning step was the same for all fossil types. 50 mg of powdered fossil samples were weighed into 15 ml polypropylene centrifuge tubes, and 7 ml of sodium bicarbonate-buffered dithionite citrate solution (Mehra and Jackson, 2013) was added to the samples. The tubes were then placed in a 80 ℃ water bath for ten minutes. This step was originally included to remove metal oxide coatings, which could potentially trap exogenous nitrogen (Mehra and Jackson, 2013; Ren et al., 2009). After cooling, samples were centrifuged, the solution was decanted, and the remaining powder was rinsed three times with 10 ml of Milli-Q water (18.2 MΩ cm, < 5 ppm TOC) and transferred to pre-combusted 4 ml glass vials.

Following our standard protocols, the oxidative cleaning was performed using recrystalized potassium persulfate for foraminifers and enamel material, sodium hypochlorite for coral samples, and perchloric acid for diatom samples. In the first protocol, a basic potassium persulfate solution consisting of 2 g of sodium hydroxide, 2 g of potassium persulfate and 100 ml of Milli-Q water was added to the foraminifera and enamel samples, which were subsequently autoclaved for 65 minutes at 120 ℃. The oxidative solution was removed by aspiration after centrifugation, and the remaining powder was rinsed four times with 4 ml Milli-Q water and dried in a clean oven at 60 ℃ for 24 hours. In the second protocol, coral samples were soaked in 4.25 ml sodium hypochlorite (10–15% available chlorine), in pre-combusted glass vials placed horizontally on a shaker table rotating at 120 rpm for 24 h. Samples were then centrifuged, the solution was removed by aspiration, and the remaining powder was rinsed three times with Milli-Q water and dried in a clean oven at 60 ℃ for 24 hours. In the third protocol, diatoms were cleaned with 7% perchloric acid in a boiling water bath for 1 hour in 15 ml polypropylene

199 centrifuge tubes, centrifuged and decanted. The remaining powder was transferred to pre-

200 combusted 40 ml glass tubes and subsequently cleaned with 60% perchloric acid in boiling water

201 bath for 2 hours, rinsed with Milli-Q water until the pH was neutral, and dried for 24-48 hours in

202 a clean oven at 60°C.

203

204 After cleaning, foraminifera, coral and enamel powder were demineralized using 4 *N*

205 hydrochloric acid, and organic N was oxidized to nitrate with a solution prepared using 0.7 g

206 recrystallized potassium persulfate, 4 ml of 6.25 *N* NaOH, and 95 ml Milli-Q water. Samples

207 were autoclaved for 65 min at 120 °C, and centrifuged. Cleaned diatoms were dissolved and the

208 organic N released from the frustules oxidized to nitrate in one step by adding 1 ml of a solution

209 prepared using 3 g of recrystallized potassium persulfate, 12 ml of 6.25 N NaOH, and 83 ml

210 Milli-Q water. Diatom samples were autoclaved at 120 °C for 95 min. For all fossil types

211 analyzed, the concentration of nitrate in the oxidized solutions was determined by

212 chemiluminescence (Braman and Hendrix, 2002). An aliquot of the nitrate solution equivalent to

213 5 nmol of N was quantitatively converted to nitrous oxide (N_2O) using the denitrifier method

214 (Sigman et al., 2001), and the $\delta^{15}N$ of the N_2O generated was determined by a purpose-built inlet

215 system coupled to a Thermo MAT253 Plus stable isotope ratio mass spectrometer (Weigand et

216 al., 2016).

217

218 International reference nitrate standards (USGS34, IAEA-NO-3) were analyzed with each batch

219 of samples and used to calculate nitrogen concentration and calibrate the isotopic composition of

220 samples *vs.* air N_2. The N content and $\delta^{15}N$ of the persulfate oxidation reaction blank was

221 measured in duplicate in each batch of samples and was used to correct the fossil-bound

222 measurements. International reference amino acid standards (USGS40 and USGS41 or USGS65)

223 were analyzed to monitor the persulfate oxidation. The N content of the blank across the

224 different batches was between 0.1 and 0.4 nmol/ml. The precision (1σ) for repeated $\delta^{15}N$

225 measurements of the untreated standards described in Section 2.1 was 0.10‰ for the MF-1

226 foraminifera standard (n=9), 0.16‰ for the MF-2 standard (n=9), 0.10‰ for the LO-1 coral

227 standard (n=9), 0.17‰ for the PO-1 coral standard (n=9), 0.11‰ for the AG-Lox tooth standard

228 (n=6), 0.28‰ for the Noto-2 tooth standard (n=3), 0.68‰ for the Hippo-1 standard (n=3), and

229 0.02‰ for the DI-1 diatom standard (n=3).

230

2.3 Experimental design

232 The experimental design is summarized in Fig. 1, and the different steps followed in each

233 experiment are described below and in the next sections. For each sample type, an aliquot of

234 uncleaned powder was taken and used in our chemical oxidation experiment. The remaining

235 powder was subsequently cleaned in four aliquots (of 50 mg each) following the reductive-

236 oxidative cleaning methods described in Section 2.2. After cleaning, the dry fossil powder was

237 combined in a single vial and homogenized. This homogenous cleaned powder was measured (at

238 least in triplicate) and used as a control sample for all our treatments. For both the dissolution

239 and the thermal degradation experiments, samples were measured twice: (1) directly after the

240 treatment, and (2) with a re-cleaning of the fossil powders after the dissolution and temperature

241 treatments.

242

243 Each treatment was performed in triplicate for all the fossil standards described in Table 1. We

244 performed a total of 413 individual measurements. The results of the experiments are reported in

245 Figures 2 to 5 and the data are available in the Supporting Information file.

246

2.3.1 Chemical oxidation experiment

248 We designed an experiment in which the different fossil samples (Table 1) were exposed to

249 consecutive oxidative cleaning steps using a solution of sodium hypochlorite (corals), basic

250 potassium persulfate (foraminifera and tooth enamel), and perchloric acid (diatoms), following

251 the methods described in Section 2.2. The first oxidation step had the objective of removing any

252 external (non-mineral-bound) organic material and is part of our standard cleaning procedure.

253 The second oxidation step was used to evaluate the potential effect of exposure to strongly

254 oxidizing conditions on the N content and isotopic composition of the remaining fossil-bound

255 organic matter. If the mineral matrix provided an effective barrier against chemical attack, we

256 would expect to see no change in N content or $\delta^{15}N$ when comparing the first and second

257 oxidative cleanings. In contrast, if the matrix was permeable, the organic matter would be

258 vulnerable to chemical attack, and we would expect a decrease in N content. In addition, if this

259 process preferentially removed ^{14}N or ^{15}N, we would expect a change in $\delta^{15}N$ and a decrease in

260 N content. In contrast, if the mineral matrix was permeable but organic material was removed

261   without any isotopic discrimination, we would expect to find a decrease in N content but no

262   change in δ^{15}N.

263

264   **2.3.2 Mineral Dissolution Experiment**

265   Artificial dissolution experiments of the calcite (foraminifera), aragonite (corals) and enamel

266   (teeth) standards were performed by adding different amounts of HCl to known quantities of the

267   standard mineral powder. We tested three treatments that resulted in around 25%, 50% and 70%

268   dissolution in corals and foraminifera, and in around 40%, 60% and 75-90% dissolution in

269   enamel (Fig. 2). Each treatment was performed in triplicate for each standard fossil material.

270   After dissolution, the remaining powder was rinsed five times with Milli-Q water and dried in a

271   clean oven at 60 ℃. The dry powder was weighed and its N isotopic composition was

272   determined using the methods described in Section 2.2. We compared the results obtained when

273   measuring the samples directly after dissolution to those obtained when the samples were re-

274   cleaned after the dissolution treatment, in order to evaluate the possibility that organic matter

275   was exposed during the dissolution but not removed during the rinsing with Milli-Q water.

276

277   For the diatom dissolution experiment, ~15-25 mg aliquots of cleaned diatom standard material

278   were placed in pre-combusted 4 ml glass vials and filled with 4 ml 0.15 M NaOH solution. The

279   vials were then placed in an 85°C water bath for ~15 min (~40% dissolution), ~1 hr (~60%

280   dissolution), and 1.5 hr (70% dissolution). In the 70% dissolution experiment, the supernatant

281   was replaced with fresh 0.15 M NaOH solution after one hour and the samples were placed back

282   in 85 °C water bath for another 0.5 hr. In all experiments, the supernatant was discarded after

283   heating, and the residual opal samples were rinsed 5 times with Milli-Q water and dried in a

284   clean oven at 60 °C for 36 hours. N isotopic composition was determined using the methods

285   described in Section 2.2.

286

287   The aim of these experiments was to compare the potential effects of partial dissolution of the

288   inorganic mineral matrix on the isotopic composition of fossil-bound organic matter. If the

289   isotopic composition of the organic N within the fossil was heterogenous and dissolution

290   preferentially affected parts of the fossil with a distinct isotopic composition, we would expect to

291   see differences in δ^{15}N between the different treatments and the untreated reference sample.

292

2.3.3 Thermal degradation experiment

294 We performed a series of laboratory experiments in which the cleaned diatom, coral,

295 foraminifera and teeth samples described in Table 1 were exposed to different temperatures (100

296 ºC, 200 ºC, 300 ºC, 400 ºC and 500 ºC) in a muffle furnace for 24 hours. Aliquots of the different

297 standard materials were placed in the muffle furnace inside 4 ml pre-combusted glass vials

298 covered with pre-combusted aluminum foil. The muffle furnace was heated from room

299 temperature to the target temperature in 1.5 hours and kept at temperature for 24 hours. Then, the

300 furnace was allowed to cool down to a temperature below 50 °C before the sample vials were

301 taken out of the furnace. The N isotopic composition of the remaining diatom, coral,

302 foraminifera, and teeth powder was measured following the procedure described in Section 2.2.

303 Similar to the dissolution experiment described in the previous section, we compared the results

304 obtained when measuring the samples directly after heating to those obtained when the samples

305 were re-cleaned after the heating treatment.

306

2.4 Statistical analysis

308 The results of the multiple measurements for each treatment in the different experiments are

309 presented as means ±1 standard deviation (panels A and B in Figs. 2 to 4, and E and F in Figs. 3

310 and 4, and all panels in Fig. 5). When calculating the difference between the control and the

311 treatment, the standard deviations of the two measurements were propagated (panels C and D in

312 Figs. 2 to 4, and G and H in Figs 3 and 4). The mean δ^{15}N values obtained after the different

313 treatments were compared to those obtained for the untreated control sample with a Student's t-

314 test. A *p*-value of < 0.01 was considered statistically significant.

315

3 Results and Discussion

3.1 Impact of chemical oxidation on fossil-bound δ^{15}N

318 Relative to the uncleaned sample, our experiments showed a significant decrease in N content

319 during the first oxidative cleaning in all the fossils analyzed, except in the diatom sample (Fig.

320 2A). The N content of the uncleaned samples was 103% higher than after the first oxidative

321 cleaning (i.e. the control sample) for the North Atlantic mixed foraminifera sample, 250% higher

322 for the Southern Ocean mixed foraminifera sample, 331% higher for the deep-sea coral, 46%

323   higher for the shallow water coral, 309% higher for the modern elephant enamel sample, 305%

324   higher for the fossil hippo enamel sample and 417% higher for the fossil suid enamel sample

325   (Fig. 2C). The N content of the uncleaned diatom sample was only 7% higher than after the first

326   oxidative cleaning, and not statistically significant. The large reduction observed in most fossil

327   types after the first cleaning was the expected result, because the purpose of this first cleaning

328   step was to remove external (non-mineral-bound) organic matter from the sample. The external

329   organic matter was likely mostly from the natural (e.g., sedimentary) environment in most cases,

330   but some of it may have derived from contamination during collection and storage.

331

332   Not surprisingly, the removal of the external organic N was associated with variable changes in

333   the isotopic composition of the different fossil types (Fig. 2B). The δ^{15}N of the North Atlantic

334   mixed foraminifera sample increased significantly by 1.25±0.16‰, but the δ^{15}N of the Southern

335   Ocean mixed foraminifera sample decreased significantly by 0.87±0.23‰ (Fig. 2D). The δ^{15}N of

336   the deep-sea coral increased significantly (by 0.67±0.11‰), while the shallow water coral δ^{15}N

337   barely changed (decreasing by 0.06±0.19‰, but not significantly), despite the substantial

338   decrease in its N content. The δ^{15}N change of the diatom sample (from 0.93±1.21‰ to

339   1.78±0.02‰) was not significant, but cleaning resulted in a drastic decrease in standard

340   deviation. Suid and hippo fossil enamel showed large increases (2.99±0.40‰ and 4.21±1.30‰,

341   respectively), but modern enamel did not show a significant change (decreasing by

342   0.22±0.15‰), despite the large reduction in its N content. The absence of significant δ^{15}N

343   changes in the modern enamel sample and the modern shallow-water coral core sample suggest

344   that most of the organic matter present in the drilled teeth material and coral core was

345   endogenous to the organism and well-preserved despite not being bound to the mineral matrix.

346   However, the significant δ^{15}N change associated with the removal of external organic material in

347   other relatively recent (i.e. Holocene) samples (e.g. deep-sea coral and the two foraminifera

348   samples) and the very large change associated with the Plio-Pleistocene fossil enamel samples

349   highlight the potential for isotopically distinct N to become associated with fossil surfaces and

350   thus the need for harsh cleaning prior to the analysis of the N isotopic composition of fossil

351   bound organic material. Whether δ^{15}N rose or fell upon cleaning could depend on multiple

352   factors, some of which may be identifiable. For example, foraminifera derive from deep sea

353   sediments, and sedimentary organic N is known to undergo a diagenetic increase in δ^{15}N

354 (Freudenthal et al., 2001; Robinson et al., 2012). However, there are a range of possible

355 influences on the $\delta^{15}N$ of the external N, which will vary with sample type and sample origin.

356 Thus, the reasons for $\delta^{15}N$ change upon cleaning are not pursued further here.

357

358 Notably, the subsequent re-oxidation of all the samples analyzed resulted negligible changes in N

359 content and isotopic composition (Fig. 3A and 3B). In fact, for all fossil types analyzed, the N

360 content and $\delta^{15}N$ of the re-oxidized samples were statistically indistinguishable from those

361 obtained after a single oxidation (Fig. 3C and 3D). These results show that the mineral matrix

362 indeed represents an effective physical barrier that protects organic matter against chemical

363 attack, even with exceptionally strong oxidizing solutions (Fig. 6A).

364

365 Our findings are in good agreement with previous experiments designed to optimize the cleaning

366 protocols of different fossil types (e.g., foraminifera, corals, teeth, otoliths or diatoms) using

367 either sodium hypochlorite or perchloric acid. In these experiments, the different fossil types

368 were exposed to the oxidizing solutions for different times, either at room temperature, or with

369 moderate heating to 60-70 °C (Kast, 2020; Lueders-Dumont et al., 2018; Ren, 2010; Sigman et

370 al., 1999). In general, all the studies showed a drop in N content and changes in $\delta^{15}N$ after a few

371 hours of exposure to the reagent, as expected from the removal of the external (non-bound)

372 organic matter. However, the N content and $\delta^{15}N$ of the sample stabilized with time, so that any

373 additional time exposure to the reagent did not change N content or isotopic composition. In

374 general, the application of heat resulted in a faster removal of the external organic matter, but did

375 not change the N content or the $\delta^{15}N$ of the fossils analyzed with respect to that of the samples

376 oxidized at room temperature. The original aim of these studies was to identify the optimal time

377 and chemical reagent for the complete removal of external organic matter, but they also provided

378 strong support for the stability of fossil-bound material.

379

380 In previous work, one exception to these uniformly straightforward findings has involved the

381 cleaning of diatom frustules. Very fresh diatom opal, such as from diatom cultures, appears to be

382 vulnerable to specific reagents, such as hydrogen peroxide (Morales et al., 2013). However,

383 diatom opal is rapidly altered in the marine environment, for example, increasing its aluminum

384 content by more than ten times upon incorporation in the sediments (Ren et al., 2013). This

385   alteration appears to "harden" the mineral to render it robust against hydrogen peroxide. Still, for

386   Holocene opal oozes from the North Pacific, there are signs that diatom microfossils might not

387   be able to protect fossil-native N against boiling perchloric acid (Brunelle et al., 2007). As

388   described below, the heating experiments from the current study may explain these earlier

389   results.

390

391   Previous work also suggests that, for diatom opal, some oxidative reagents and treatments can be

392   too weak to fully remove externally vulnerable N, which required extensive testing to settle on

393   the current cleaning protocol (Brunelle et al., 2007; Robinson et al., 2004). In contrast, for

394   carbonate and phosphate biominerals, reagent choices (e.g., persulfate *vs.* hypochlorite) have

395   shown little to no influence (Kast, 2020; Leichliter et al., 2021; Lueders-Dumont et al., 2018;

396   Ren et al., 2009; Straub, 2012), albeit with a recrystallization-related exception for the otoliths of

397   one fish species (Lueders-Dumont et al., 2018). We suspect that this difference of diatom opal

398   from calcium carbonate and phosphate minerals relates to the unique and mutable characteristics

399   of diatom opal, as will be discussed further in the context of the heating experiments in Section

400   3.3.

401

402   Our oxidant exposure experiments were, of course, not conducted on the geologic time scale, i.e.,

403   over thousands to millions of years. In this and other regards, the experiments are not an ideal

404   simulation of the exposure of fossil material to sedimentary diagenesis. However, the oxidants

405   used were far more aggressive than those used by microbes to attack sedimentary organic matter.

406   Thus, our findings are strongly supportive of the view that fossil-bound N is well protected by

407   the mineral matrix from the external environment, supporting the argument that fossil-bound N

408   preserves the $\delta^{15}N$ of fossil-native organic matter generated by ancient organisms.

409

410   **3.2 Impact of biomineral dissolution on foram-, coral-, tooth enamel- and diatom-bound**

411   **$\delta^{15}N$**

412   In our first set of experiments, samples were measured directly after the dissolution treatment

413   (left panels in Fig. 3). The results of this first experiments showed a progressive increase in N

414   content per mg of mineral as we increased the percentage of dissolved mineral matrix (Fig. 3A

415   and 3C). The observed N increase during the most aggressive treatment was smaller for tooth

416 enamel than for marine fossils (Fig. 3A). However, the N content of the untreated teeth samples
417 was higher than that of the foraminifera and corals, although it was lower than that of the
418 diatoms. In net, the proportional N content increase found in the most aggressive treatment was
419 similar for foraminifera (20-34%) and corals (21-22%), slightly higher for tooth enamel (32-
420 42%) samples, and substantially lower for diatoms (2%) (Fig. 3C). The observed N content
421 increase from the most aggressive treatment was statistically significant compared to the
422 untreated sample for all the fossil types, except for the diatom sample.

423

424 The observed increase in N content during dissolution could indicate that: (i) organic matter
425 exposed during the dissolution experiment was not completely removed by rinsing multiple
426 times with Milli-Q water, or (ii) dissolution preferentially occurred in N-poor parts of the
427 mineral matrixes. In order to test these two hypotheses, we repeated the dissolution experiment,
428 but introducing a second oxidative cleaning step after the dissolution treatment (right panels in
429 Fig. 3). If the increase in N content was caused by incomplete removal of organic matter exposed
430 during dissolution, we would expect that this organic matter would be removed during this
431 additional oxidative cleaning. However, if it was caused by dissolution of N-poor regions of the
432 fossils, we would expect that the increasing N content trend will persist after the additional
433 cleaning. Our results show that after the second cleaning, for all of the fossils except for the
434 shallow water coral, the N content of the fossils analyzed after the different dissolution
435 treatments was statistically undistinguishable from the untreated control sample. These results
436 clearly indicate that the N increase observed in the first experiment for most of the fossil types
437 was due to incomplete removal of organic matter that was exposed during the dissolution
438 treatment; and, consequently, they confirm that the dissolution did not have a significant
439 preference for N-rich or N-poor biomineral.

440

441 In contrast, for the shallow water coral, there was a similar decrease (of 16-20%) during all
442 dissolution treatments relative to the undissolved sample. For this sample, an argument can be
443 made that the first dissolution (of ~25%) did access N-rich skeletal material. The decline in N
444 content was relatively constant with respect to the fraction dissolved, which may indicate the
445 dissolution of a discrete N-rich biomineral component, as opposed to dissolution being guided by
446 a continuous range in biomineral N content. Scleractinian coral skeleton is observed to contain

447   microcrystalline septa that are associated with the onset of calcification (the "rapid accretion

448   deposits", also referred to as "centers of calcification"), representing ~5% of the skeleton

449   (Stolarski, 2003). Spatially-resolved measurements indicate that the rapid accretion deposits are

450   microcrystalline and richer in organics as well as non-calcium cations than the "thickening

451   deposits", the main skeletal component (Cuif and Dauphin, 2005). There is also evidence that the

452   rapid accretion deposits are the first component to undergo diagenesis and recrystallization

453   (Frankowiak et al., 2013). Thus, there are both conceptual and observational expectations that

454   this material would be particularly vulnerable to acid dissolution. Accordingly, the 16-20%

455   decline in N content of the coral sample under any level of acid addition in our experiments may

456   reflect the nearly complete dissolution of this microcrystalline component.

457

458   Despite the differences in N content found in most fossil types between our two versions of the

459   dissolution experiment (i.e., with and without subsequent oxidative cleaning), our results indicate

460   that the effect of partial dissolution on δ^{15}N was minimal in both cases (Fig. 3E to 3H). In most

461   of the fossils, the difference between the acid treatments and the untreated samples was within

462   0.3‰ (Fig. 3G and 3H), i.e. within 1-2 standard deviations of the typical analytical precision of

463   the method (see Section 2.2).

464

465   We first consider the implications of the second experiment (with subsequent oxidative

466   cleaning), which is the better analogue for actual samples. In this experiment, the lack of change

467   in dissolved relative to undissolved samples indicates that the dissolution did not preferentially

468   remove isotopically distinct N (Fig. 6). This is not surprising. For isotopic change to have

469   occurred, there would need to be both (i) distinct solubilities among components of the

470   biomineral and (ii) isotopic differences that correlate with the susceptibility to dissolution. Our

471   results show very little change in N content, already arguing that N content variations, if they

472   occur at all, are not strongly correlated with biomineral variation. Otherwise, the comparison of

473   our two experiments confirm that any N exposed by the dissolution process is successfully

474   removed by our fossil cleaning.

475

476   Turning to the first experiment (i.e., without subsequent oxidative cleaning), beyond the

477   conclusions stated above, the N content increases indicate that a portion of the N exposed during

478   dissolution has an adequately robust structural (biochemical) framework to remain attached at

479   the biomineral surface during repeated rinsing of the sample with Milli-Q water (Fig. 6).

480   However, the δ^{15}N results indicate that this now-superficial N was not greatly changed in δ^{15}N

481   by the dissolution process. This, again, is not surprising. Peptide bond hydrolysis could induce

482   significant isotopic fractionation (Bada et al., 1989). However, protein hydrolysis requires much

483   higher acid/base concentrations and temperatures, and longer reaction times (Roach and Gehrke,

484   1970). Accordingly, in our experiments, some N could be exhumed and survive the dissolution

485   on the mineral surface, without undergoing clear isotopic changes in the process. Most of the

486   data are consistent with this scenario.

487

488   We now turn to the few isotopic changes that were observed. In our first experiment (i.e.,

489   without subsequent oxidative cleaning), the biggest difference in δ^{15}N with respect to the

490   untreated samples (-0.96±0.49‰) was observed after the 87% dissolution treatment of one of our

491   fossil enamel samples (Fig. 3E and 3G). This treatment also resulted in one of the largest

492   increases in N content (42%) with respect to the untreated sample. However, due to the relatively

493   large standard deviation in δ^{15}N obtained for replicate analysis of the fossil, this difference was

494   not statistically significant. The large standard deviation obtained for the untreated sample, and

495   across the different treatments, suggests a more heterogenous isotopic composition for this

496   particular fossil. Interestingly, in the case of the modern enamel sample, dissolution treatments

497   up to 91% resulted in negligible changes in δ^{15}N values, despite of the large increase in N

498   content (32%) relative to the untreated sample. The diatom sample showed one of the lowest

499   changes in δ^{15}N (0.15±0.03‰) during the most aggressive treatment (69% dissolution).

500   Paradoxically, this difference was statistically significant with respect to the untreated sample

501   due to the extremely low standard deviation of the diatom replicate measurements. The only

502   other sample that showed a statistically significant difference (0.56±0.21‰) was the shallow

503   water coral sample when dissolved by 47-70%. The differences observed in all the other coral,

504   foraminifera and teeth fossils were statistically indistinguishable from the untreated samples.

505

506   In our second experiment (i.e., with subsequent oxidative cleaning), the difference between the

507   different dissolution treatments and the untreated samples were even smaller (Fig. 3F and 3H). In

508   contrast to the first experiment, the shallow-water coral sample was undistinguishable from the

509 control sample in all the treatments. However, the deep-water coral sample exposed to 70%

510 dissolution showed a statistically significant difference (0.59±0.15‰) with respect to the

511 untreated sample. Unfortunately, we could not perform the second experiment for the suid fossil

512 enamel sample nor for the diatom sample because no sample powder was left. Nevertheless, the

513 rest of the fossil samples analyzed, including an additional Plio-Pleistocene fossil enamel

514 sample, were indistinguishable from the untreated samples (Fig. 3F and 3H). We consider this

515 second experiment more directly comparable to environmental samples that were exposed to

516 dissolution in the past, because any fossil-native organic matter that might have been exposed

517 during dissolution would be removed by our standard cleaning protocol and not measured.

518

519 The fact that the δ^{15}N of the diatom and the deep-sea coral samples exposed to ~70% dissolution

520 were statistically different from the untreated sample is not particularly concerning for the

521 application of the fossil-bound δ^{15}N method. The diatom samples were isolated from deep-sea

522 sediment cores. Thus, they have already undergone substantial dissolution in the water column

523 and sediments as part of normal diagenetic processes (Van Cappellen et al., 2002). The ~70%

524 further dissolution would thus represent an extreme degree of dissolution relative to the starting

525 diatom opal material. Despite this situation, the observed δ^{15}N changes were very small

526 (0.15±0.03‰) and would not significantly impact the palaeoceanographic interpretation. The

527 deep-sea coral δ^{15}N increase (of 0.59±0.15‰) at 75% dissolution applied only to the dissolution

528 experiment that included subsequent cleaning (Fig. 3H *vs*. 3G), which raises questions about its

529 robustness. On the other hand, deep-sea corals record extensive periods of time and can capture

530 major δ^{15}N changes (Wang et al., 2014), so the sample might be more heterogeneous and thus

531 vulnerable to preferential loss of isotopically distinct material.

532

533 In summary, the stability of δ^{15}N after the different dissolution treatments indicate a generally

534 uniform isotopic composition for foraminifera-, coral-, enamel-, and diatom-bound organic

535 material, and imply that the N exposed during dissolution is lost without significant isotopic

536 discrimination (Fig. 6). This conclusion is also supported by the similarity in the isotopic

537 composition observed in our two experiments (with/without subsequent oxidative cleaning)

538 despite significant differences in N content (Figs 3G and 3H). More practically, the second

539 experiment indicates that the partial dissolution of fossil opal, calcite, aragonite or enamel

540   matrixes has a negligible effect on the N content and N isotopic composition of fossil-bound

541   organic matter. These results are consistent with those obtained in a foraminifera δ^{15}N ground-

542   truthing field study near Bermuda, which suggest that foraminifera-bound N loss during early

543   seafloor diagenesis does not occur with significant isotope fractionation because any newly

544   exposed N is completely lost rather than isotopically altered (Smart et al., 2018).

545

546   In addition, our dissolution experiment results provide a framework for understanding the effect

547   of calcite recrystallization in marine sediments. A remarkable finding from the study of early

548   Cenozoic planktonic foraminifera-bound δ^{15}N is that the fossil-bound N content and δ^{15}N are

549   preserved (Kast et al., 2019) despite the evidence for substantial recrystallization and isotopic

550   resetting of the foraminifer tests in deep sea sediments (Killingley, 1983; Pearson et al., 2001;

551   Pearson et al., 2007). Our results indicate that the organic matter exposed by acid dissolution, at

552   least in part, remains physicochemically connected with the surface of the remaining biomineral.

553   Considering that the dissolution–reprecipitation of foraminiferal calcite is fast and occurs at a

554   small spatial scale (Chanda et al., 2019), we hypothesize that the "exposed" organic N could be

555   re-encapsulated in the recrystallized biomineral before it is lost or altered by bacterial attack.

556

557

558   **3. 3 Impact of thermal decomposition on fossil-bound δ^{15}N**

559   As with the dissolution experiments, our first set of thermal degradation experiments samples

560   were measured directly after the heating treatment, without a subsequent oxidative recleaning

561   (left panels in Fig. 4). Our results showed no significant change in N content for all fossil types

562   at 100 ºC and 200 ºC, except for diatoms (Figs. 4A and 4C). At temperatures > 200 ºC, deep and

563   shallow water aragonitic coral samples showed a progressive decrease in N content of 12% and

564   42%, respectively, at 300 ºC, 49% and 59% at 400 ºC, and 80% and 79% at 500 ºC. In contrast,

565   the two calcitic mixed foraminifera samples showed no significant N losses at 300 ºC, only a

566   moderate decreased at 400 ºC (15% and 27%), and a large decline at 500 ºC (80% and 82%).

567   Interestingly, at 400 ºC, the decline observed in the foraminifera was substantially smaller than

568   the one found in the corals, but, at 500 ºC, N losses were comparable for both fossil types.

569   Finally, the N content of the modern and fossil enamel samples was statistically indistinguishable

570   from that of the untreated samples up to 400 ºC, and decreased by only 33% at 500 ºC in the

571   fossil sample, while there was not statistically significant N loss from the modern enamel

572   sample. Thus, tooth enamel is an interesting contrast with the ~80% reduction in calcitic

573   foraminifera and aragonitic corals. These results indicate that the fraction of N lost at different

574   temperatures depends on the mineral structure (and thus the mineral composition) of the fossil.

575

576   The effect of the different thermal treatments on the isotopic composition of fossil-bound N also

577   varied widely across the different fossil types analyzed (Fig. 4E and 4G). All fossils, except the

578   diatoms, showed negligible changes in δ^{15}N at 100 °C. At 200 °C, deep-sea corals increased with

579   respect to the untreated samples by 0.52±0.17‰, and the two foraminifera samples by

580   0.41±015‰ and 0.75±0.18‰, respectively, but the shallow water corals and the teeth samples

581   showed no significant changes (Fig. 4G). At 300 °C, deep-sea and shallow water coral δ^{15}N

582   increased moderately by 1.10±0.20 ‰ and 0.75±0.19‰, respectively. In contrast, the δ^{15}N

583   increase observed in the two foraminifera samples (0.62±0.14‰ and 0.75±0.25‰) was

584   undistinguishable from the one observed at 200 °C, while the two tooth enamel samples

585   continued to show no significant change. At 400 °C, the δ^{15}N increase observed for the deep and

586   shallow corals (1.12±0.24‰ and 0.74±0.30‰), and the two foraminifera samples (0.67±0.16‰

587   and 0.95±0.16‰) was undistinguishable from that observed at 300 °C. Again, the two tooth

588   enamel samples did not show any significant δ^{15}N change. Finally, at 500 °C, the δ^{15}N increase

589   of the deep-sea coral (1.83±0.37‰) and the two foraminifera samples (3.19±0.32‰ and

590   3.57±0.49‰) was significantly higher than in the experiment performed at 400 °C, and coincided

591   with substantial N loss, of about 80%. However, the δ^{15}N of the shallow water coral dropped to

592   values similar to those found in the untreated sample, despite a similar N loss. As in the previous

593   treatments, the two tooth enamel samples did not show any significant change at 500 °C. Thus,

594   our results reveal that both the N loss and the degree of isotopic change at different temperatures

595   is directly linked to the mineral composition of the fossil.

596

597   In order to investigate further the relationship between N loss and δ^{15}N changes, we estimate the

598   isotope effect of thermal decomposition of fossil bound organic material. The isotope effect (ε)

599   expresses the degree of isotopic discrimination and is commonly defined as the ratio of reaction

600   rates at which the two isotopes are converted from reactant to product (i.e., ε (‰) = ((1- ^{15}k/^{14}k)

601   × 1000); where ^{x}k is the rate constant for the ^{x}N-containing reactant). We use the slope of the

602   correlation of δ^{15}N against the natural logarithm of the N content to obtain a Rayleigh model-

603   based estimate of the net isotope effect   associated with the loss of N caused by thermal

604   decomposition of fossil bound organic material (upper panels in Fig. 5) (e.g. Fripiat et al. (2019).

605   If we plot our results across the entire temperature range (0-500 ºC), we obtain a significant

606   correlation for the two foraminifera samples and deep-sea coral, but not for the shallow water

607   coral and the teeth samples (Fig 5A). However, the correlation for the shallow water coral

608   sample was significantly improved if the 500 ºC treatment was excluded (Fig. 5B). In the 0-400

609   ºC range, the correlation for the deep-sea coral sample was still significant, but it was not for the

610   foraminifera samples. In the 0-300 ºC range, the correlation was only significant for the shallow

611   water coral sample. Interestingly, the estimated isotope effects for the two coral samples were

612   relatively similar (ranging from -0.80‰ to -1.04‰) across the 0-500 ºC and 0-400 ºC

613   temperature ranges, suggesting that the isotopic discrimination during thermal degradation was

614   relatively similar at different temperatures for aragonitic samples. The isotope effects from the

615   two foraminifera samples were also very similar to one another (-1.76‰ and -1.22‰),

616   suggesting a slightly higher isotope effect for calcite than for aragonite. Finally, as expected from

617   the lack of variability in N content and δ^{15}N, the correlation for the two teeth samples was not

618   significant across any of the temperature ranges analyzed. Thus, our results raise the possibility

619   that the isotope effects during thermal degradation of fossil bound organic matter are different

620   for aragonite, calcite and apatite samples.

621

622   As an alternative possibility, there may be isotopically distinct forms of N that are preferentially

623   lost and retained that could explain or contribute to isotopic changes. In this case, the similar

624   isotope effects observed for different biominerals could relate more to the organisms producing

625   the fossil-bound N rather than the biomineral itself. Our strongest argument against this

626   alternative interpretation is that nearly all regressions yield a weak negative (or insignificant)

627   slope, which would seem unlikely if the isotopic changes were driven by preferential loss of

628   specific N forms in different types of organisms.

629

630   During this first set of experiment, the behavior of the diatom sample was not consistent with the

631   rest of the fossils and/or with expectations from thermal degradation of frustule bound organic

632   matter. Our results showed substantial increases in N content (~300%) with respect to the

633   untreated sample at 100 ℃, suggesting substantial contamination of the frustule material with

634   exogenous N (Fig. 4A and 4C). This N content increase was accompanied by a significant

635   reduction in δ^{15}N values (of 2.56‰) (Fig. 4E and 4G). This contamination problem persisted at

636   higher temperatures, and the N content of the treated samples at 200 ℃ and 300 ℃ was still

637   higher (and the δ^{15}N significantly lower) than that of the untreated control sample. A mass

638   balance of the N change between the control sample and the 100 ℃ measurements reveals that

639   δ^{15}N of the N added was 0.28‰. The ability of diatom opal to adsorb N species has been noted

640   previously (Robinson et al., 2004), and it also appears to apply to carbon species (Zheng et al.,

641   2002). We have not as yet investigated further the mechanism or form of the opal N

642   contamination. However, we suspect that it derives from some of the same characteristics of

643   diatom opal that also lead to the unique sensitivity of diatom-bound δ^{15}N to the cleaning

644   protocol, as discussed in section 3.1. The high effective surface area of opal and its potential for

645   chemical and structural transformation upon heating (e.g, associated with opal dehydration) may

646   allow for the exposure, alteration, and release of diatom-native N, as well as uptake of exogenous

647   N species, close to the opal surface. In any case, these results indicate that heated diatom opal

648   requires recleaning to remove adsorbed N.

649

650   As with our investigation of partial dissolution, we performed a second set of heating

651   experiments in which an oxidative recleaning step was added after the heating treatment (right

652   panels in Fig. 4). This second experiment allowed us to further investigate: (i) the effect of N

653   absorption into the opal, and (ii) to what extent the observed changes in δ^{15}N in the different

654   treatments involved the organic matter that remained bound within the mineral or only organic

655   matter that could have been exposed during heating. As in the case of the dissolution

656   experiments, any adsorbed or exposed organic material would be removed during the second

657   oxidative cleaning, allowing us to analyze only the fraction of organic material that remained

658   protected within the biomineral matrix. An additional motivation for this suite of experiments is

659   that they better address the situation of fossil-bound N isotopic analysis of naturally heated

660   samples because fossil samples are always cleaned before they are measured.

661

662   In this second set of experiments, the observed N content trends were, in general, very similar to

663   those obtained in our first set of experiments for all fossil types, except for the diatoms (Fig. 4B

664 and 4D). These findings indicate that the additional cleaning step did not remove a substantial

665 amount of organic matter that was exposed during heating but that remained on the surface of the

666 fossil material. This indicates that the organic matter exposed by heating is subsequently almost

667 completely lost from the fossil material. This is not surprising because, at temperatures > 300 ºC,

668 we would expect that the exposed organic material would be combusted and thus volatilized into

669 the air.

670

671 Nevertheless, we observe a few small, but in some cases significant, differences in the $\delta^{15}N$

672 trends of some fossils between the "un-recleaned" and "recleaned" heating experiments. These

673 differences suggest that some small amount of organic matter was exposed and altered during

674 heating and was subsequently removed during the recleaning (Fig. 6C). The removed N was

675 probably too small to be detected in our N content measurements, but its isotopic composition

676 may have been different enough to slightly change the $\delta^{15}N$ of the fossils in some cases. In

677 particular, in the recleaned experiment, the $\delta^{15}N$ of the two foraminifera standards was

678 indistinguishable from the reference in the range from 100 ºC to 400 ºC, and it was only

679 statistically different at 500 ºC, indicating that foraminifera calcite was stable up to 400 ºC. The

680 two coral standards showed similar trends as in the un-recleaned experiment, but the difference

681 with respect to the reference sample was smaller, particularly for the deep-sea coral. As in the

682 un-recleaned experiments, the modern and fossil enamel samples showed no significant change

683 in the range of temperatures analyzed, but the fossil enamel showed larger increases at 400 ºC

684 (0.91±0.35‰), and 500 ºC (0.73±0.31‰), suggesting that it may be less robust than modern

685 enamel. Regarding the calculated isotope effects (Fig. 5), overall, they were somewhat smaller

686 than those obtained in the un-recleaned experiment, suggesting that the values obtained in the

687 un-recleaned experiments may slightly overestimate the fractionation induced by thermal

688 removal of fossil-bound N. This may be due to more intense isotopic alteration of organic N that

689 is exposed but not removed during the heating treatment. It is worth noting that the isotope

690 effects obtained for foraminifera and corals were very low (typically < 1‰), indicating that the

691 potential biases introduced by thermal alteration would be small even if they result in significant

692 N loss (> 90%), as observed at 500 ºC.

693

694   In contrast to the similar trends observed for rest of the fossils in both sets of experiments, the

695   diatom sample showed a very different pattern when it was re-cleaned after the heating

696   treatment, suggesting that the additional cleaning step did effectively remove the adsorbed N that

697   contaminated the samples in the first experiment. In the re-cleaned heating experiment, diatoms

698   showed no significant change in N content or δ^{15}N at 100 ºC (Fig. 4D and 4H). At 200 ºC, they

699   indicated a small but statistically significant reduction in N content (15%), accompanied by a

700   0.92±0.04‰ increase in δ^{15}N. At temperatures > 200 ºC, the diatom sample showed the greatest

701   decrease in N content of all the fossil types analyzed, with declines of 58% at 300 ºC, 94% at 400

702   ºC, and 99% at 500 ºC. This sharp decrease in N content was accompanied by large changes in

703   δ^{15}N. At 300 ºC, diatom δ^{15}N increased with respect to the untreated control sample by

704   4.44±0.06‰, and at 400 ºC, it increased by 5.46±0.15‰. In contrast, at 500 ºC, diatoms showed

705   a somewhat smaller increase in δ^{15}N than at 400 ºC and 300 ºC, despite of the 99% decrease in

706   its N content. Consistent with these observations, the isotope effect for the diatom sample varied

707   substantially, ranging from -5.33‰ between the control sample and 300 ºC to -0.99‰ between

708   the control and 500 ºC (Fig. 5D to 5F). These results may suggest the removal of different types

709   of frustule-bound organic matter at different temperatures, with different isotopic compositions

710   and/or different isotope effects applying to each type. However, the nearly complete loss of the

711   initial diatom-bound N at the highest temperatures argues for caution in interpreting these results.

712   Overall, the patterns observed in diatom N content and δ^{15}N are consistent with those obtained

713   with other fossils, albeit with a much greater magnitude, and support the observation that both

714   the N loss and the degree of isotopic change at different temperatures are directly linked to the

715   robustness of the mineralogy and structure of the fossil.

716

717   Thermogravimetric analysis of pretreated *Pinnularia* diatom frustules has shown that substantial

718   sample weight loss associated with the removal of the organic fraction of the frustule starts to

719   occur at temperatures between 200 ºC and 300 ºC, and continues until 550 ºC, above which no

720   further decrease in weight is detected (Van Eynde et al., 2014). Biogenic aragonite (from

721   powdered *Acropora* corals) starts to transform to calcite at 280 ºC, and is completely transformed

722   to calcite at 380 ºC (Yoshioka and Kitano, 1985). Substantial calcite decomposition typically

723   begins between 500 ºC and 550 ºC, although marine carbonates may already become unstable at

724   temperatures between 400 ºC and 500 ºC due to the presence of magnesium (Hirota and Szyper,

725   1975). Tooth enamel suffers structural and chemical alteration in response to thermal stress

726   mainly at temperatures > 600 ºC (Robinson and Kingston, 2020; Shipman et al., 1984).

727

728   These ranges of decomposition temperatures for opal, aragonite, calcite and enamel are

729   consistent with the temperatures at which we start to observe substantial N loss and δ^{15}N changes

730   in diatoms, corals, foraminifera and tooth enamel samples. The observation of significant N

731   content and δ^{15}N changes in diatoms already at 200 ºC, and the fast rate of N loss indicate that

732   the frustule material becomes permeable to N at high temperatures. The N loss and associated

733   δ^{15}N change observed in coral samples at 300 ºC was likely associated with the conversion of

734   aragonite to calcite. However, the smaller proportional change in N content observed between

735   300 ºC and 400 ºC suggest that part of the coral-bound N was still trapped in the newly forming

736   calcite. The subsequent N loss and δ^{15}N change observed at 500 ºC was consistent with the one

737   observed in the calcitic foraminifera samples, and it was likely associated with the

738   decomposition of calcite in both cases. Finally, the absence of significant changes in N content

739   and isotopic composition of modern enamel up to 500 ºC is consistent with minor alteration of

740   the matrix at this temperature. However, the changes observed in fossil tooth enamel at 400 ºC

741   and 500 ºC suggest that enamel may become less robust to thermal stress with aging.

742

743   Our results, when compared to these temperatures for biomineral modification, suggest that the

744   mineral matrix of the fossil acts as a nearly closed system with respect to N, up to the point that

745   heating compromises the integrity of the mineral matrix itself (Fig. 6C). Previous studies have

746   shown that in *Porites* coral powder heated under aqueous conditions at 80 ºC, 110 ºC and 140 ºC,

747   the amino acid concentrations in the supernatant water remained within the analytical limit of

748   detection despite of substantial changes in the chemical composition of intra-crystalline amino

749   acids, indicating that the carbonate skeleton retained this organic N pool (Tomiak et al., 2013).

750   Our new experiments are consistent with these observations and indicate that not only amino

751   acids but also total N is retained within the mineral matrix at temperatures of 100 ºC in all the

752   fossil types analyzed. Hence, our results indicate a negligible effect of thermal degradation on

753   fossil-bound organic matter N isotopic composition in the range of temperatures associated with

754   local geothermal gradients in Cenozoic marine sediments, which are typically < 60 ºC

755   (Malinverno and Martinez, 2015). In addition, our data reveal that, in some cases (e.g., calcite or

756 enamel), N can remain isotopically unaltered within the mineral matrix even at temperatures well
757 above the typical combustion temperatures of protein amino acids, which range from 185 ℃ to
758 280 ℃ (Weiss et al., 2018). These findings suggest that the fossil-bound N isotope method could
759 be applied in enamel, calcitic and even aragonitic fossil samples that have suffered substantial
760 thermal stress without significant biases on the reconstructed δ^{15}N values. However, further work
761 is required to fully explore this possibility.

762

763 Our observations may also help to explain some previous observations regarding the sensitivity
764 of diatom-bound δ^{15}N to the cleaning protocol used. It has been noted that diatom opal from
765 particularly opal-rich sediments, which tends to have a lower Al/Si ratio (Ren et al., 2013), has
766 diatom-bound N that is vulnerable to δ^{15}N alteration by boiling in perchloric acid (Brunelle et al.,
767 2007; Robinson et al., 2004). Moreover, this effect appears to be absent in diatom opal from
768 glacial-age samples, in which the opal has a higher Al/Si ratio (Brunelle et al., 2007; Ren et al.,
769 2013). The temperature of boiling perchloric acid is greater than 100 °C, increasing with
770 dehydration. Our temperature treatment experiments indicate that diatom frustules can both lose
771 and gain N, due to thermal modification of the diatom opal above 100 ℃. Thus, the previous
772 findings regarding diatom cleaning may be explained by the effect of treatment temperature on
773 the structural integrity of the diatom opal.

774

775 **4 Conclusions**

776
777 Our experiments performed under controlled laboratory conditions indicate the following.

778

779   (i) Fossil-bound organic matter is effectively isolated by the mineral matrix from chemical
780   changes in the surrounding environment.
781   (ii) Fossil-bound organic matter is completely removed without isotopic discrimination after
782   partial dissolution of the mineral matrix.
783   (iii) Fossil-bound organic matter has a relatively uniform N isotopic composition across the
784   mineral matrix.
785   (iv) The fossil-native organic matter exposed by acid dissolution remains, at least in part, as a
786   physicochemical framework connected with the remaining biomineral. If recrystallization

787   occurs at a scale that minimizes exposure of this organic N to microbes, our observations offer

788   a possible explanation for the apparent stability of fossil-bound organic matter in

789   recrystallized biominerals.

790   (v) During heating, the mineral matrix behaves as a nearly closed system with respect to N, up

791   to the point that the high temperature compromises the integrity of the mineral matrix itself.

792

793   Thus, our results provide strong experimental support for the robustness of fossil-bound organic

794   matter to reconstruct the original N isotopic composition of ancient organisms. We acknowledge

795   that the full range of diagenetic reactions found in the environment on geological timescales are

796   difficult to simulate in the laboratory. Thus, direct observations from the geologic past are also

797   necessary to provide a more complete assessment of the potential diagenetic effects on fossil

798   bound organic matter. In this vein, the results obtained here are consistent with observations

799   from the geologic past. First, a number of studies have shown that the N content of fossils

800   remains relatively stable across thousands to millions of years, suggesting that mineral matrix

801   acted as a closed system with respect to N (Kast et al., 2019; Leichliter et al., 2021; Ren et al.,

802   2017; Studer et al., 2012). Second, different species of foraminifera, which have different

803   sensitivities to alteration of the mineral matrix, reveal consistent δ^{15}N changes (Ren et al., 2017;

804   Ren et al., 2015; Straub et al., 2013). Third, foraminifera, corals and diatoms, which have

805   different sensitivities to alteration, provide consistent estimates of regional δ^{15}N changes when

806   measured across the same time periods and in the same regions (Ai et al., 2020; Martinez-Garcia

807   et al., 2014; Studer et al., 2015; Wang et al., 2017).

808

809   The evidence, reported here and previously, for the robustness of fossil-bound N has

810   implications from prior comparisons of fossil-bound and bulk sediment δ^{15}N, which often shows

811   dramatic differences (Martinez-Garcia et al., 2014; Ren et al., 2017; Robinson et al., 2005;

812   Straub et al., 2013; Studer et al., 2021). Bulk sediment δ^{15}N is known to be sensitive to

813   diagenetic alteration and contamination by terrestrial N inputs (Robinson et al., 2012). In

814   contrast, so long as the diagenetic conditions are appropriate to preserve the biomineral in

815   question, fossil-bound δ^{15}N appears to be remarkably robust. Even in situations of biomineral

816   recrystallization, such as in early Cenozoic, carbonate-rich deep-sea sediments, N content and

817   δ^{15}N data indicate the preservation of fossil-bound N (Kast et al., 2019), which is consistent with

818   the results of the dissolution experiments presented here. Thus, the comparison of fossil-bound

819   and bulk sediment $\delta^{15}N$ could offer insights into diagenetic processes affecting sedimentary

820   organic matter through time, or into changes in terrestrial N inputs. Alternatively, if one seeks to

821   argue that the fossil-bound N is "to blame" for a disagreement with bulk sediment $\delta^{15}N$, or if

822   differences in fossil-bound-$\delta^{15}N$ are found among different fossil types or species, one must look

823   to the biological controls on the isotopic signatures incorporated into fossil-bound organic matter

824   by the fossil-producing organisms. This situation motivates an expansion of ground-truthing

825   research that focuses on the biological and ecological controls on the N encapsulated within

826   different types of newly generated biominerals.

827

832

833   **Author contribution**

834   A.M-G designed the experiments, supervised the analysis of the samples and wrote the

835   manuscript, with feedback from D.M.S. J.J. performed the experiments on, and measured the

836   isotopic composition of the coral, foraminifera and tooth enamel standards. X.E.A performed the

837   experiments on, and measured the isotopic composition of the diatom standard. N.D. and A.F.

838   prepared the coral standards and were involved in the analytical training of J.J. T.W. was

839   involved in the characterization of the coral standards. A.A. prepared the foraminifera standards.

840   F.F., S.M. and X.E.A. prepared the diatom standards. JL and TL prepared the tooth enamel

841   standards. All authors were involved in the discussion of the data at different stages of the

842   project and contributed to the final version of the manuscript.

843

844   **Open Research**

845   **Data Availability Statement**

846   All the data generated in this study are available in the Supporting Information.
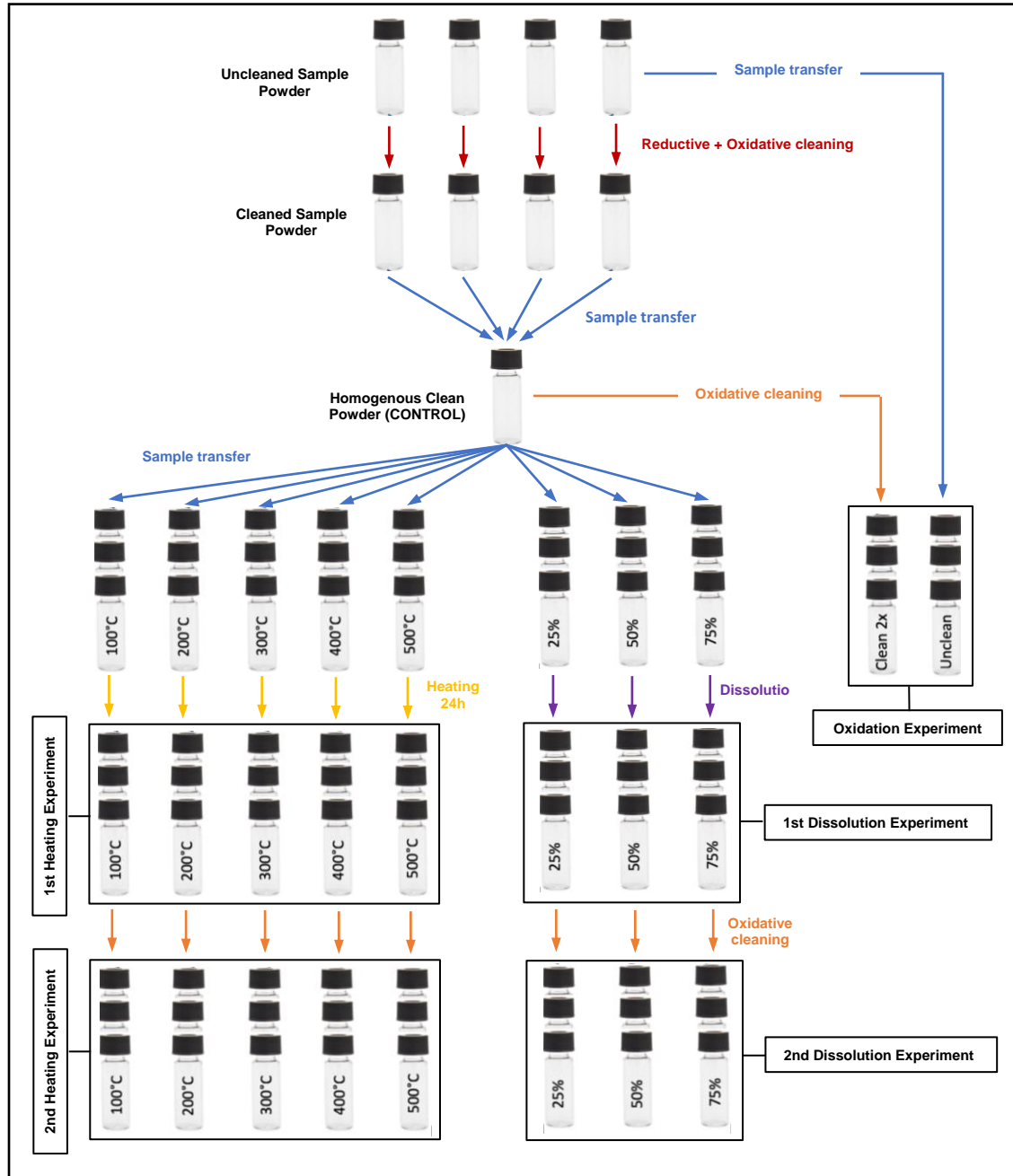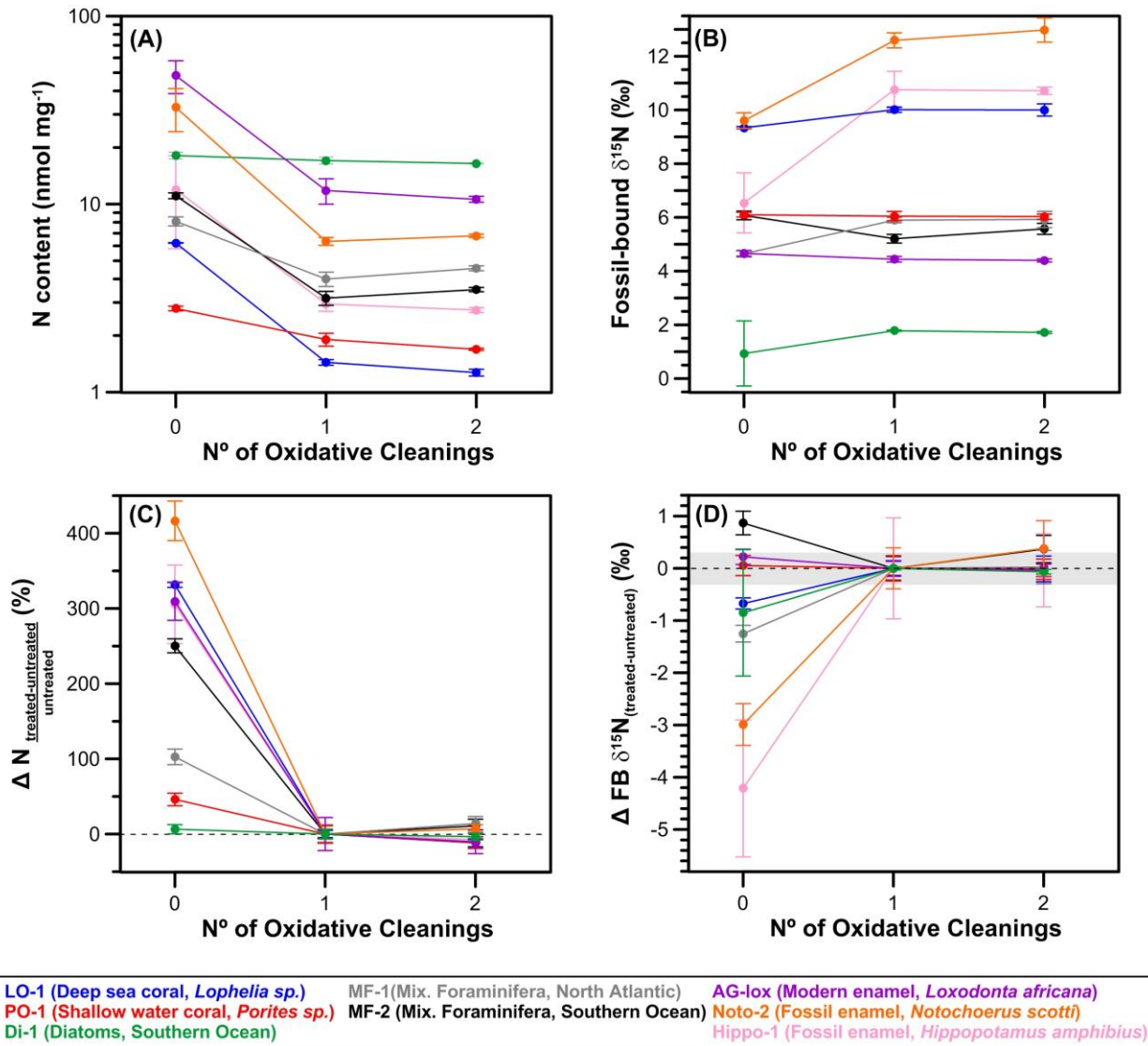
847

848   **Figures:**
849

850
851
852   **Figure 1. Experimental Design.** For each sample type, an aliquot of uncleaned powder was
853   taken and used in our chemical oxidation experiment. The remaining powder was subsequently
854   cleaned in four aliquots (of 50 mg each) following the reductive-oxidative cleaning methods
855   described in Section 2.2. After cleaning, the dry fossil powder was combined in a single vial and
856   homogenized. This homogenous cleaned powder was measured (at least in triplicate) and used as
857   a control sample for all our treatments. In our oxidation experiment, the uncleaned sample
858   aliquot was measured in triplicate and compared to our control sample, and to an aliquot of the
859   control sample that was oxidatively re-cleaned in triplicate. In our dissolution experiments, we

860 performed three triplicate treatments in which around 25%, 50% and 75% of the control sample
861 was dissolved. In our first dissolution experiment the sample powders remaining after dissolution
862 were rinsed five times with Milli-Q water and measured. While, in our second experiment the
863 powders were re-cleaned oxidatively before the measurement. In our heating experiments, the
864 control sample powder was heated to 100 ºC, 200 ºC, 300 ºC, 400 ºC and 500 ºC. In our first
865 experiment samples were measured directly after heating, while in our second experiment
866 samples were re-cleaned oxidatively before the measurement.
867

868

869
870

871 **Figure 2. Evaluation of the effect of exposure to strongly oxidative conditions on fossil-**
872 **bound δ^{15}N**. Effect of consecutive oxidative cleanings with solutions of bleach (corals),
873 potassium peroxydisulphate (foraminifera and teeth) and perchloric acid (diatoms) on fossil-
874 bound (A) N content and (B) δ^{15}N. Notice that in (A) a log$_{10}$ scale is used in the Y axis to
875 facilitate comparison of the different fossil types. (C) Percent N content difference of 0
876 oxidations and 2 oxidations with respect to the 1 oxidation treatment. (D) Same difference as in
877 (C) but for δ^{15}N instead of percent N content. The grey shaded area highlights differences
878 between the treated and untreated samples that are within 0.3‰. In (A) and (B) error bars
879 represent the 1 sigma standard deviation of triplicate oxidation experiments performed for each
880 treatment (see Fig. 1). In C and D error bars indicate the propagated uncertainty from A and B,
881 respectively. Note that the untreated reference sample in this experiment is the sample that has
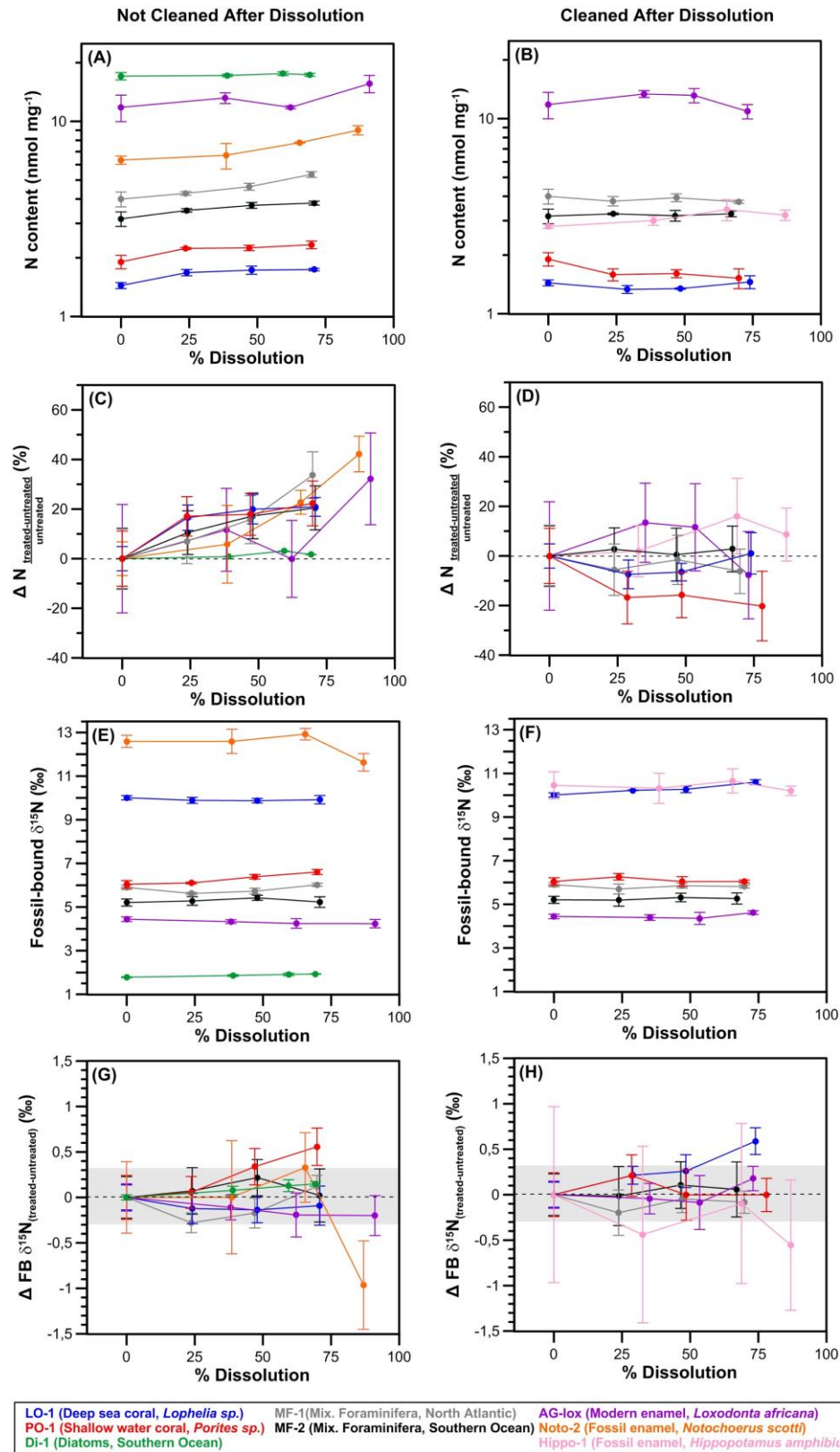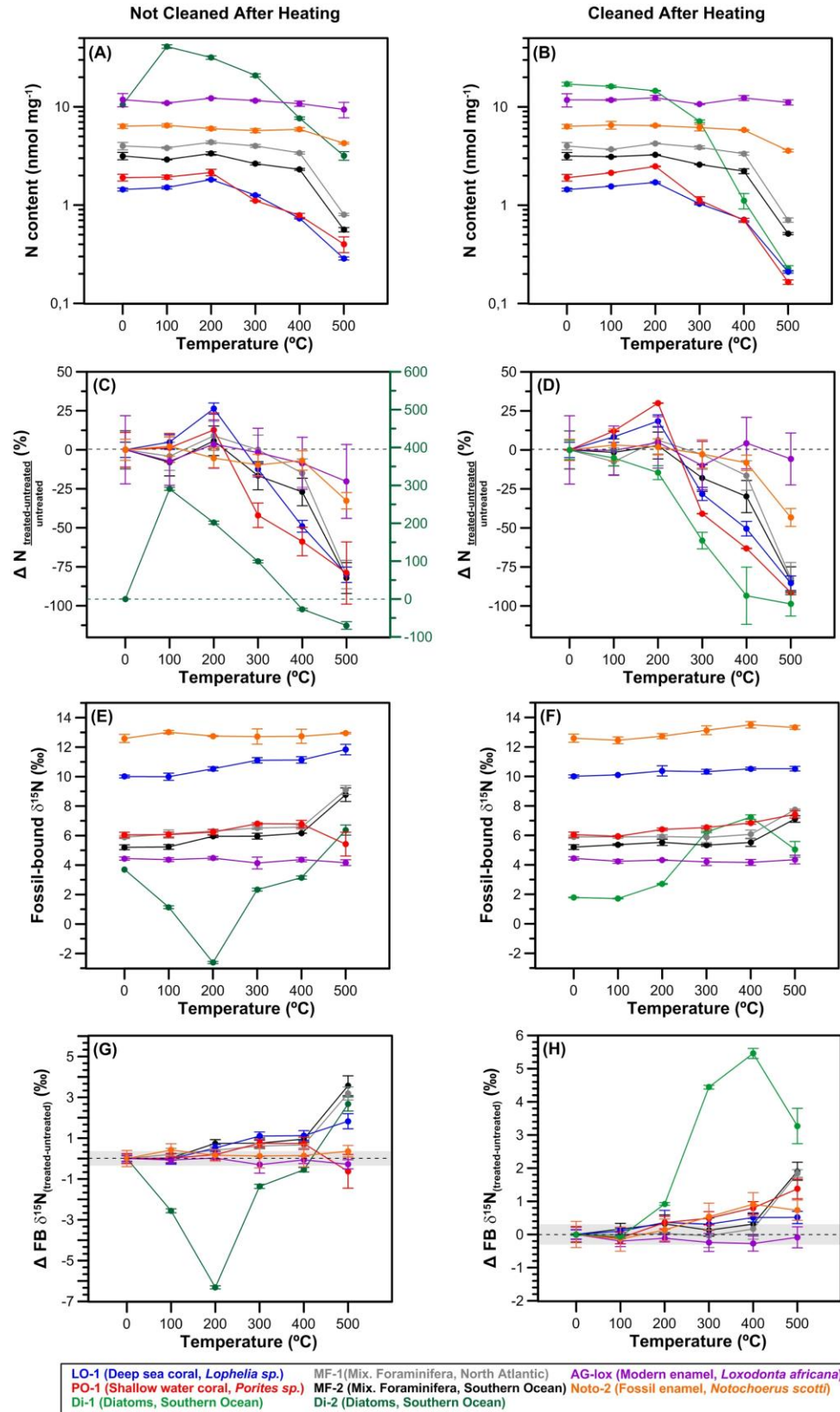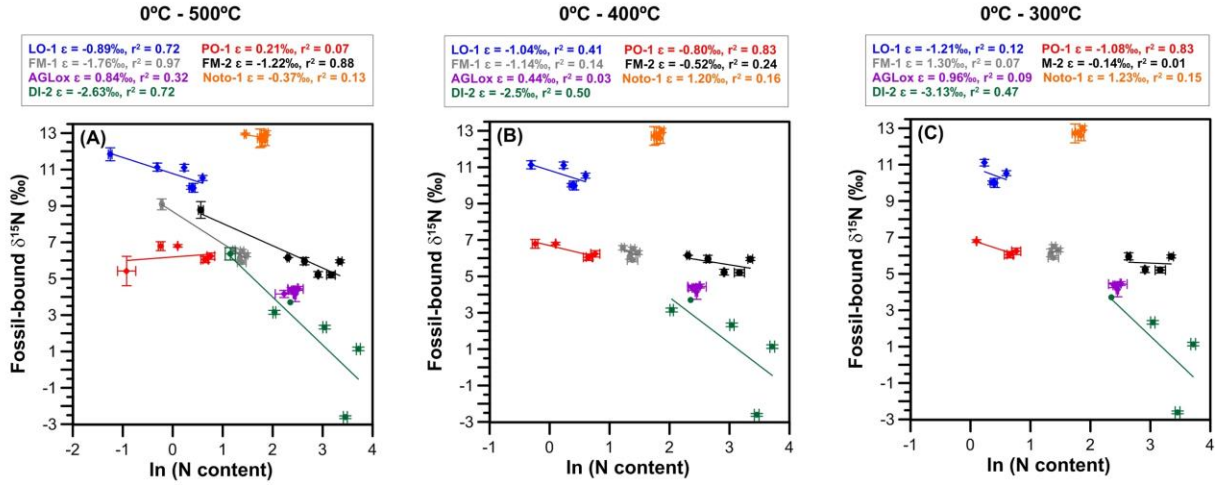882 been cleaned once, and not the uncleaned sample.

883

Not Cleaned After Dissolution   **Cleaned After Dissolution**

LO-1 (Deep sea coral, *Lophelia sp.*)   MF-1(Mix. Foraminifera, North Atlantic)   AG-lox (Modern enamel, *Loxodonta africana*)
PO-1 (Shallow water coral, *Porites sp.*)   MF-2 (Mix. Foraminifera, Southern Ocean)   Noto-2 (Fossil enamel, *Notochoerus scotti*)
Di-1 (Diatoms, Southern Ocean)   Hippo-1 (Fossil enamel, *Hippopotamus amphibius*)

Figure 3. Evaluation of the effect of biomineral dissolution on fossil-bound δ^{15}N. Left panels (A, C, E, G) show results for samples measured directly after the dissolution treatment. Right

889   panels (B, D, F, and H) show results for samples that were subjected to an additional oxidative
890   cleaning after the dissolution treatment. (A, B) N content and (E, F) $\delta^{15}N$ of different fossil
891   types. Notice that in (A and B) a $\log_{10}$ scale is used in the Y axis to facilitate comparison of the
892   different fossil types. (C, D) Percent N content difference between each dissolution treatment
893   and the untreated sample. (G, H) $\delta^{15}N$ difference between each dissolution treatment and the
894   untreated sample. The grey shaded area highlights differences between the treated and untreated
895   samples that are within 0.3‰. In (A, B, E and F) error bars represent the 1 sigma standard
896   deviation of triplicate dissolution experiments performed for each treatment (see Fig. 1). In C, D,
897   G, and H error bars indicate the propagated uncertainty from A, B, E and F, respectively.
898

Figure 4. Evaluation of the effect of heating on fossil-bound δ^{15}N. Left panels (A, C, E, G) show results for samples measured directly after the heating treatment. Right panels (B, D, F,

903 and H) show results for samples that were subjected to an additional oxidative cleaning after the
904 heating treatment. (A, B) N content and (E, F) $\delta^{15}N$ of different fossil types. Notice that in (A
905 and B) a $\log_{10}$ scale is used in the Y axis to facilitate comparison of the different fossil types. (C,
906 D) Percent N content difference between each heating treatment and the untreated sample.
907 Notice that in C, percent N content values for the DI-2 sample are plotted in the right axis. (G,
908 H) $\delta^{15}N$ difference between each heating treatment and the untreated sample. The grey shaded
909 area highlights differences between the treated and untreated samples that are within 0.3‰. In
910 (A, B, E and F) error bars represent the 1 sigma standard deviation of triplicate heating
911 experiments performed for each treatment (see Fig. 1). In C, D, G, and H error bars indicate the
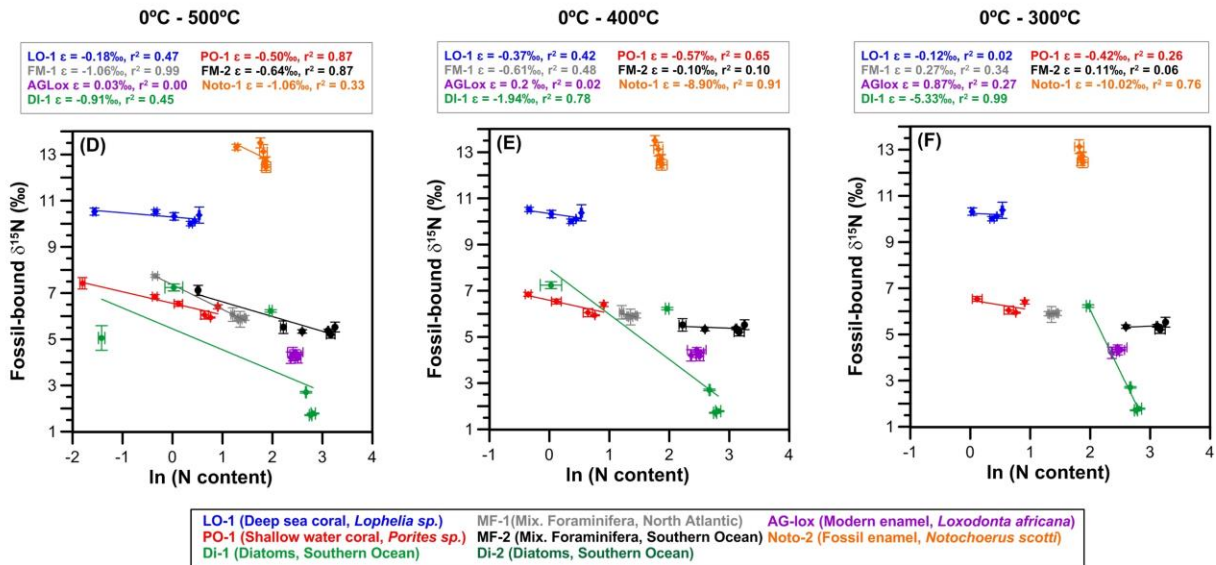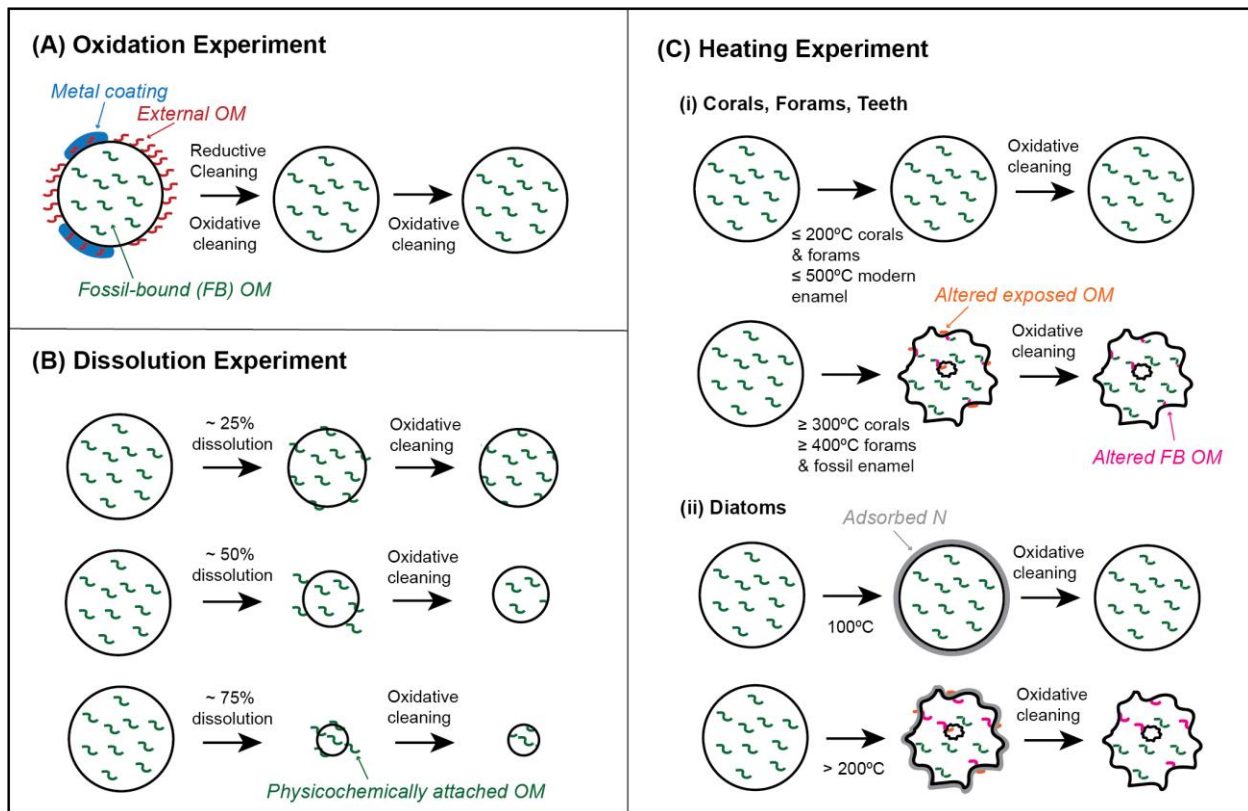912 propagated uncertainty from A, B, E and F, respectively.

913
914

Figure 5. Evaluation of the isotope effect associated with thermal degradation of fossil-bound δ^{15}N. Upper panels (A, B, C) show results for samples measured directly after the heating treatment. Lower panels (D, E, F) show results for samples that were subjected to an additional oxidative cleaning after the heating treatment. The figure shows fossil-bound δ^{15}N *vs* the natural logarithm (ln) of the N content for the different temperature treatments shown in Fig 4. (A) Considering data from the entire temperature range (0 ℃ to 500 ℃), (B) from 0 ℃ to 400 ℃, and (C) from 0 ℃ to 300 ℃. The slope of the linear regressions (indicated above each plot) provides an estimate of the isotope effect (ε) associated with the loss of N from the fossil (see text). Error bars represent the 1 sigma standard deviation of triplicate experiments performed for each treatment.

927

928

929
930
931
932 **Figure 6. Diagram summarizing the interpretation of the oxidation, dissolution and heating**
933 **experiments.** Black lines indicate the boundary of the mineral particles. Red lines symbolize
934 external (non-bound) organic matter (OM). Blue area denotes metal coatings around the
935 biomineral surface, which may contain external OM. Continuous green lines represent fossil
936 bound (FB) organic structures. Dashed green lines indicate FB-OM that may have changed its
937 molecular structure (but not its $\delta^{15}N$) due to heating. Orange lines represent organic matter that
938 was exposed and altered (in its $\delta^{15}N$ composition) during heating. Pink lines represent OM that
939 was altered in its $\delta^{15}N$ composition during heating, but remained bound to the biomineral after
940 oxidative recleaning. Grey lines represent N species that adsorb to the mineral during heating.
941 (A) Our oxidation experiments show a substantial reduction in N content and variable changes in
942 $\delta^{15}N$ after our reductive and oxidative cleaning steps (Fig. 2C and 2D), which we interpret to
943 reflect the removal of external OM (red lines). However, the oxidative recleaning did not
944 produce any significant changes in N content or $\delta^{15}N$, indicating that FB-OM (green lines) was
945 effectively protected from chemical attack by the biomineral. (B) Our experiments reveal a
946 progressive increase in N content per mg of calcite as dissolution increased (Fig. 3C). This
947 change in N content occurred without substantial changes in $\delta^{15}N$ (Fig. 3G). The progressive
948 increase in N disappeared after an additional oxidative cleaning (Fig. 3D), without any
949 substantial change in $\delta^{15}N$ (Fig. 3 H). These results indicate that part of the FB-OM was exposed
950 after dissolution, but it was not altered, and remained physiochemically attached to the
951 biomineral (exposed green lines). This OM was not removed during rinsing with Milli-Q water,
952 but was completely eliminated with an oxidative recleaning. The stability of the $\delta^{15}N$ values

953 obtained before and after the recleaning demonstrated that FB-OM had a relatively homogenous
954 isotopic composition, and that it was not altered during the dissolution process. (C) Our results
955 indicate no significant changes in FB N content or δ^{15}N at temperatures ≤ 200 ºC in any of the
956 corals, foraminifers or teeth analyzed before and after oxidative cleaning (Fig. 4C, 4D, 4G, and
957 4H). These results indicate that despite of potential changes in the molecular structure of the FB-
958 OM (dashed green lines) that could be induced by heating (Tomiak et al., 2013), the biomineral
959 acted as a closed system with respect to N. Corals showed substantial N content changes at
960 temperatures ≥ 300 ºC, foraminifers and fossil enamel at ≥ 400 ºC, while modern enamel
961 remained stable even at 500 ºC (Fig. 4C and D). Despite of the large change in N content, after
962 oxidative cleaning the δ^{15}N of corals, forams and fossil teeth showed minimal changes (Fig. 4H).
963 This suggests that the proportion of altered FB-OM that remained in the samples (pink lines) was
964 very small. Diatoms show a very different behavior than the rest of the fossils during heating.
965 When they were not oxidatively re-cleaned after heating, N content increased and δ^{15}N decreased
966 significantly (Fig. 4C and 4G), suggesting contamination of the samples by adsorption of N
967 during heating. This contamination was successfully removed after recleaning (Fig. 4D). In
968 contrast to the other fossil types, in diatoms, substantial N loss was observed already at
969 temperatures ≥ 200 ºC, and it was associated with substantial δ^{15}N changes (Fig. 4C and 4G).
970 These findings suggest the presence of a larger proportion of altered FB-OM (pink lines) in
971 diatoms than in other fossil after heating. Overall, our results indicate that N loss depends on the
972 resistance of the biomineral itself to thermal stress, and also that the potential alteration of FB-
973 OM was minimal for corals, foraminifers and teeth, but was significant for diatoms, at
974 temperatures ≥ 200 ºC.
975

References:

Ai, X.E., Studer, A.S., Sigman, D.M., Martínez-García, A., Fripiat, F., Thöle, L.M.*, et al.* (2020) Southern Ocean upwelling, Earth's obliquity, and glacial-interglacial atmospheric CO_2 change. *Science* 370, 1348-1352. doi:10.1126/science.abd2115

Altabet, M.A. and Curry, W.B. (1989) Testing models of past ocean chemistry using foraminifera15N/14N. *Global Biogeochemical Cycles* 3, 107-119. doi:10.1029/GB003i002p00107

Bada, J.L., Schoeninger, M.J. and Schimmelmann, A. (1989) Isotopic fractionation during peptide bond hydrolysis. *Geochim. Cosmochim. Acta* 53, 3337-3341. doi:10.1016/0016-7037(89)90114-2

Bai, Y., Yu, Z., Ackerman, L., Zhang, Y., Bonde, J., Li, W.*, et al.* (2020) Protein nanoribbons template enamel mineralization. *Proceedings of the National Academy of Sciences* 117, 19201-19208. doi:10.1073/pnas.2007838117

Braman, R.S. and Hendrix, S.A. (2002) Nanogram nitrite and nitrate determination in environmental and biological materials by vanadium(III) reduction with chemiluminescence detection. *Analytical Chemistry* 61, 2715-2718. doi:10.1021/ac00199a007

Bridoux, M.C., Annenkov, V.V., Keil, R.G. and Ingalls, A.E. (2012a) Widespread distribution and molecular diversity of diatom frustule bound aliphatic long chain polyamines (LCPAs) in marine sediments. *Organic Geochemistry* 48, 9-20. doi:10.1016/j.orggeochem.2012.04.002

Bridoux, M.C., Keil, R.G. and Ingalls, A.E. (2012b) Analysis of natural diatom communities reveals novel insights into the diversity of long chain polyamine (LCPA) structures involved in silica precipitation. *Organic Geochemistry* 47, 9-21. doi:10.1016/j.orggeochem.2012.02.010

Brown, S.J. and Elderfield, H. (1996) Variations in Mg/Ca and Sr/Ca ratios of planktonic foraminifera caused by postdepositional dissolution: Evidence of shallow Mg-dependent dissolution. *Paleoceanography* 11, 543-551. doi:10.1029/96pa01491

Brunelle, B.G., Sigman, D.M., Cook, M.S., Keigwin, L.D., Haug, G.H., Plessen, B.*, et al.* (2007) Evidence from diatom-bound nitrogen isotopes for subarctic Pacific stratification during the last ice age and a link to North Pacific denitrification changes. *Paleoceanography* 22. doi:10.1029/2005pa001205

Burdige, D.J. (2006) Geochemistry of Marine Sediments. Princeton University Press.

Cappellini, E., Welker, F., Pandolfi, L., Ramos-Madrigal, J., Samodova, D., Rüther, P.L.*, et al.* (2019) Early Pleistocene enamel proteome from Dmanisi resolves Stephanorhinus phylogeny. *Nature* 574, 103-107. doi:10.1038/s41586-019-1555-y

Casciotti, K.L. (2016) Nitrogen and Oxygen Isotopic Studies of the Marine Nitrogen Cycle. *Annu Rev Mar Sci* 8, 379-407. doi:10.1146/annurev-marine-010213-135052

Castiblanco, G.A., Rutishauser, D., Ilag, L.L., Martignon, S., Castellanos, J.E. and Mejía, W. (2015) Identification of proteins from human permanent erupted enamel. *European Journal of Oral Sciences* 123, 390-395. doi:10.1111/eos.12214

Chanda, P., Gorski, C.A., Oakes, R.L. and Fantle, M.S. (2019) Low temperature stable mineral recrystallization of foraminiferal tests and implications for the fidelity of geochemical proxies. *Earth Planet. Sci. Lett.* 506, 428-440. doi:10.1016/j.epsl.2018.11.011

Cowie, G.L. and Hedges, J.I. (1994) Biochemical indicators of diagenetic alteration in natural organic matter mixtures. *Nature* 369, 304-307. doi:10.1038/369304a0

Cuif, J.-P. and Dauphin, Y. (2005) The two-step mode of growth in the scleractinian coral skeletons from the micrometre to the overall scale. *Journal of Structural Biology* 150, 319-331. doi:10.1016/j.jsb.2005.03.004

Dauwe, B. and Middelburg, J.J. (1998) Amino acids and hexosamines as indicators of organic matter degradation state in North Sea sediments. *Limnology and Oceanography* 43, 782-798. doi:10.4319/lo.1998.43.5.0782

Deniro, M.J. and Epstein, S. (1981) Influence of Diet on the Distribution of Nitrogen Isotopes in Animals. *Geochim. Cosmochim. Acta* 45, 341-351. doi:Doi 10.1016/0016-7037(81)90244-1

Duprey, N.N., Wang, X.T., Kim, T., Cybulski, J.D., Vonhof, H.B., Crutzen, P.J.*, et al.* (2020) Megacity development and the demise of coastal coral communities: evidence from coral skeleton δ^{15}N records in the Pearl River estuary. *Global Change Biology*. doi:10.1111/gcb.14923

Engel, M.H., Goodfriend, G.A., Qian, Y.R. and Macko, S.A. (1994) Indigeneity of Organic-Matter in Fossils - a Test Using Stable-Isotope Analysis of Amino-Acid Enantiomers in Quaternary Mollusk Shells. *Proceedings of the National Academy of Sciences of the United States of America* 91, 10475-10478. doi:DOI 10.1073/pnas.91.22.10475

Engel, M.H. and Macko, S.A. (1986) Stable Isotope Evaluation of the Origins of Amino-Acids in Fossils. *Nature* 323, 531-533. doi:DOI 10.1038/323531a0

Erler, D.V., Farid, H.T., Glaze, T.D., Carlson-Perret, N.L. and Lough, J.M. (2020) Coral skeletons reveal the history of nitrogen cycling in the coastal Great Barrier Reef. *Nat Commun* 11. doi:10.1038/s41467-020-15278-w

Erler, D.V., Wang, X.C.T., Sigman, D.M., Scheffers, S.R., Martinez-Garcia, A. and Haug, G.H. (2016) Nitrogen isotopic composition of organic matter from a 168 year-old coral skeleton: Implications for coastal nutrient cycling in the Great Barrier Reef Lagoon. *Earth Planet. Sci. Lett.* 434, 161-170. doi:10.1016/j.epsl.2015.11.023

Farmer, J.R., Sigman, D.M., Granger, J., Underwood, O.M., Fripiat, F., Cronin, T.M.*, et al.* (2021) Arctic Ocean stratification set by sea level and freshwater inputs since the last ice age. *Nat Geosci* 14, 684-689. doi:10.1038/s41561-021-00789-y

Frankowiak, K., Mazur, M., Gothmann, A.M. and Stolarski, J. (2013) Diagenetic Alteration of Triassic Coral from the Aragonite Konservat-Lagerstatte in Alakir Cay, Turkey: Implications for Geochemical Measurements. *Palaios* 28, 333-342. doi:10.2110/palo.2012.p12-116r

Freudenthal, T., Wagner, T., Wenzhöfer, F., Zabel, M. and Wefer, G. (2001) Early diagenesis of organic matter from sediments of the eastern subtropical Atlantic: evidence from stable nitrogen and carbon isotopes. *Geochim. Cosmochim. Acta* 65, 1795-1808. doi:10.1016/s0016-7037(01)00554-3

Fripiat, F., Martínez-García, A., Fawcett, S.E., Kemeny, P.C., Studer, A.S., Smart, S.M.*, et al.* (2019) The isotope effect of nitrate assimilation in the Antarctic Zone: Improved estimates and paleoceanographic implications. *Geochim. Cosmochim. Acta* 247, 261-279. doi:10.1016/j.gca.2018.12.003

Fripiat, F., Martínez-García, A., Marconi, D., Fawcett, S.E., Kopf, S.H., Luu, V.H.*, et al.* (2021) Nitrogen isotopic constraints on nutrient transport to the upper ocean. *Nat Geosci*. doi:10.1038/s41561-021-00836-8

1067   Gehler, A., Tutken, T. and Pack, A. (2012) Oxygen and carbon isotope variations in a modern
1068   rodent community - implications for palaeoenvironmental reconstructions. *Plos One* 7,
1069   e49531. doi:10.1371/journal.pone.0049531
1070   Hirota, J. and Szyper, J.P. (1975) Separation of total particulate carbon into inorganic and
1071   organic components1. *Limnology and Oceanography* 20, 896-900.
1072   doi:10.4319/lo.1975.20.5.0896
1073   Kast, E.R. (2020) Development and application of biogenic mineral-bound nitrogen isotope
1074   measurements to the million-year timescale, Geosciences Department. Princeton
1075   University, Princeton, NJ.
1076   Kast, E.R., Stolper, D.A., Auderset, A., Higgins, J.A., Ren, H., Wang, X.T.*, et al.* (2019)
1077   Nitrogen isotope evidence for expanded ocean suboxia in the early Cenozoic. *Science* 364,
1078   386-389. doi:10.1126/science.aau5784
1079   Killingley, J.S. (1983) Effects of diagenetic recrystallization on $^{18}O/^{16}O$ values of deep-sea
1080   sediments. *Nature* 301, 594-597. doi:10.1038/301594a0
1081   Knapp, A.N., Sigman, D.M. and Lipschultz, F. (2005) N isotopic composition of dissolved
1082   organic nitrogen and nitrate at the Bermuda Atlantic time-series study site. *Global
1083   Biogeochemical Cycles* 19. doi:Artn Gb1018
1084   10.1029/2004gb002320
1085   Kroger, N. (2002) Self-Assembly of Highly Phosphorylated Silaffins and Their Function in
1086   Biosilica Morphogenesis. *Science* 298, 584-586. doi:10.1126/science.1076221
1087   Kroger, N., Deutzmann, R., Bergsdorf, C. and Sumper, M. (2000) Species-specific polyamines
1088   from diatoms control silica morphology. *Proceedings of the National Academy of Sciences*
1089   97, 14133-14138. doi:10.1073/pnas.260496497
1090   Kullmer, O. (2008) The fossil suidae from the Plio-Pleistocene Chiwondo Beds of northern
1091   Malawi, Africa. *Journal of Vertebrate Paleontology* 28, 208-216. doi:10.1671/0272-
1092   4634(2008)28[208:Tfsftp]2.0.Co;2
1093   Leichliter, J.N., Lüdecke, T., Foreman, A.D., Duprey, N.N., Winkler, D.E., Kast, E.R.*, et al.*
1094   (2021) Nitrogen isotopes in tooth enamel record diet and trophic level enrichment: Results
1095   from a controlled feeding experiment. *Chemical Geology* 563, 120047.
1096   doi:10.1016/j.chemgeo.2020.120047
1097   Lueders-Dumont, J.A., Wang, X.T., Jensen, O.P., Sigman, D.M. and Ward, B.B. (2018) Nitrogen
1098   isotopic analysis of carbonate-bound organic matter in modern and fossil fish otoliths.
1099   *Geochim. Cosmochim. Acta* 224, 200-222. doi:10.1016/j.gca.2018.01.001
1100   Malinverno, A. and Martinez, E.A. (2015) The effect of temperature on organic carbon
1101   degradation in marine sediments. *Sci Rep* 5, 17861. doi:10.1038/srep17861
1102   Martinez-Garcia, A., Sigman, D.M., Ren, H.J., Anderson, R.F., Straub, M., Hodell, D.A.*, et al.*
1103   (2014) Iron Fertilization of the Subantarctic Ocean During the Last Ice Age. *Science* 343,
1104   1347-1350. doi:10.1126/science.1246848
1105   McCorkle, D.C., Martin, P.A., Lea, D.W. and Klinkhammer, G.P. (1995) Evidence of a
1106   dissolution effect on benthic foraminiferal shell chemistry: $\delta^{13}C$, Cd/Ca, Ba/Ca, and Sr/Ca
1107   results from the Ontong Java Plateau. *Paleoceanography* 10, 699-714.
1108   doi:10.1029/95pa01427
1109   Mehra, O.P. and Jackson, M.L. (2013) Iron Oxide Removal from Soils and Clays by a
1110   Dithionite–Citrate System Buffered with Sodium Bicarbonate, Clays and Clay Minerals,
1111   pp. 317-327.

1112 Morales, L.V., Sigman, D.M., Horn, M.G. and Robinson, R.S. (2013) Cleaning methods for the
1113   isotopic determination of diatom-bound nitrogen in non-fossil diatom frustules. *Limnol*
1114   *Oceanogr-Meth* 11, 101-112. doi:10.4319/lom.2013.11.101
1115 Pearson, P.N. (2017) Oxygen Isotopes in Foraminifera: Overview and Historical Review. *The*
1116   *Paleontological Society Papers* 18, 1-38. doi:10.1017/s1089332600002539
1117 Pearson, P.N., Ditchfield, P.W., Singano, J., Harcourt-Brown, K.G., Nicholas, C.J., Olsson, R.K.,
1118   *et al.* (2001) Warm tropical sea surface temperatures in the Late Cretaceous and Eocene
1119   epochs. *Nature* 413, 481-487. doi:10.1038/35097000
1120 Pearson, P.N., van Dongen, B.E., Nicholas, C.J., Pancost, R.D., Schouten, S., Singano, J.M. and
1121   Wade, B.S. (2007) Stable warm tropical climate through the Eocene Epoch. *Geology* 35.
1122   doi:10.1130/g23175a.1
1123 Rejebian, V.A., Harris, A.G. and Huebner, J.S. (1987) Conodont color and textural alteration: An
1124   index to regional metamorphism, contact metamorphism, and hydrothermal alteration.
1125   *Geological Society of America Bulletin* 99. doi:10.1130/0016-
1126   7606(1987)99<471:Ccataa>2.0.Co;2
1127 Ren, H. (2010) Developement and paleoceanographic application of plancktonic foraminifera-
1128   bound nitrogen isotopes, Department of Geoscience. Princeton University, Princeton, NJ.
1129 Ren, H., Sigman, D.M., Martínez-García, A., Anderson, R.F., Chen, M.-T., Ravelo, A.C., *et al.*
1130   (2017) Impact of glacial/interglacial sea level change on the ocean nitrogen cycle.
1131   *Proceedings of the National Academy of Sciences* 114, E6759-E6766.
1132   doi:10.1073/pnas.1701315114
1133 Ren, H., Sigman, D.M., Meckler, A.N., Plessen, B., Robinson, R.S., Rosenthal, Y. and Haug,
1134   G.H. (2009) Foraminiferal Isotope Evidence of Reduced Nitrogen Fixation in the Ice Age
1135   Atlantic Ocean. *Science* 323, 244-248. doi:10.1126/science.1165787
1136 Ren, H.J., Brunelle, B.G., Sigman, D.M. and Robinson, R.S. (2013) Diagenetic aluminum uptake
1137   into diatom frustules and the preservation of diatom-bound organic nitrogen. *Mar. Chem.*
1138   155, 92-101. doi:10.1016/j.marchem.2013.05.016
1139 Ren, H.J., Studer, A.S., Serno, S., Sigman, D.M., Winckler, G., Anderson, R.F., *et al.* (2015)
1140   Glacial-to-interglacial changes in nitrate supply and consumption in the subarctic North
1141   Pacific from microfossil-bound N isotopes at two trophic levels. *Paleoceanography* 30,
1142   1217-1232. doi:10.1002/2014pa002765
1143 Roach, D. and Gehrke, C.W. (1970) The hydrolysis of proteins. *Journal of Chromatography A*
1144   52, 393-404. doi:10.1016/s0021-9673(01)96589-6
1145 Robinson, J.R. and Kingston, J.D. (2020) Burned by the fire: Isotopic effects of experimental
1146   combustion of faunal tooth enamel. *Journal of Archaeological Science: Reports* 34.
1147   doi:10.1016/j.jasrep.2020.102593
1148 Robinson, R.S., Brunelle, B.G. and Sigman, D.M. (2004) Revisiting nutrient utilization in the
1149   glacial Antarctic: Evidence from a new method for diatom-bound N isotopic analysis.
1150   *Paleoceanography* 19. doi:10.1029/2003pa000996
1151 Robinson, R.S., Kienast, M., Luiza Albuquerque, A., Altabet, M., Contreras, S., De Pol Holz, R.,
1152   *et al.* (2012) A review of nitrogen isotopic alteration in marine sediments.
1153   *Paleoceanography* 27. doi:10.1029/2012pa002321
1154 Robinson, R.S., Sigman, D.M., DiFiore, P.J., Rohde, M.M., Mashiotta, T.A. and Lea, D.W.
1155   (2005) Diatom-bound N-15/N-14: New support for enhanced nutrient consumption in the
1156   ice age subantarctic. *Paleoceanography* 20. doi:10.1029/2004pa001114

Rosenthal, Y., Lohmann, G.P., Lohmann, K.C. and Sherrell, R.M. (2000) Incorporation and preservation of Mg inGlobigerinoides sacculifer:implications for reconstructing the temperature and18O/16O of seawater. *Paleoceanography* 15, 135-145. doi:10.1029/1999pa000415

Schroeder, R.A. (1975) Absence of β-alanine and γ-aminobutyric acid in cleaned foraminiferal shells: Implications for use as a chemical criterion to indicate removal of non-indigenous amino acid contaminants. *Earth Planet. Sci. Lett.* 25, 274-278. doi:10.1016/0012-821x(75)90241-1

Shemesh, A., Macko, S.A., Charles, C.D. and Rau, G.H. (1993) Isotopic Evidence for Reduced Productivity in the Glacial Southern Ocean. *Science* 262, 407-410. doi:10.1126/science.262.5132.407

Shipman, P., Foster, G. and Schoeninger, M. (1984) Burnt Bones and Teeth - an Experimental-Study of Color, Morphology, Crystal-Structure and Shrinkage. *J Archaeol Sci* 11, 307-325. doi:Doi 10.1016/0305-4403(84)90013-X

Sigman, D.M., Altabet, M.A., Francois, R., McCorkle, D.C. and Gaillard, J.F. (1999) The isotopic composition of diatom-bound nitrogen in Southern Ocean sediments. *Paleoceanography* 14, 118-134. doi:Doi 10.1029/1998pa900018

Sigman, D.M., Casciotti, K.L., Andreani, M., Barford, C., Galanter, M. and Bohlke, J.K. (2001) A bacterial method for the nitrogen isotopic analysis of nitrate in seawater and freshwater. *Analytical Chemistry* 73, 4145-4153. doi:DOI 10.1021/ac010088e

Sigman, D.M. and Fripiat, F. (2019) Nitrogen Isotopes in the Ocean, Encyclopedia of Ocean Sciences, pp. 263-278.

Sigman, D.M., Fripiat, F., Studer, A.S., Kemeny, P.C., Martínez-García, A., Hain, M.P.*, et al.* (2021) The Southern Ocean during the ice ages: A review of the Antarctic surface isolation hypothesis, with comparison to the North Pacific. *Quat. Sci. Rev.* 254, 106732. doi:10.1016/j.quascirev.2020.106732

Smart, S.M., Ren, H., Fawcett, S.E., Schiebel, R., Conte, M., Rafter, P.A.*, et al.* (2018) Ground-truthing the planktic foraminifer-bound nitrogen isotope paleo-proxy in the Sargasso Sea. *Geochim. Cosmochim. Acta* 235, 463-482. doi:10.1016/j.gca.2018.05.023

Smith, A.C., Leng, M.J., Swann, G.E.A., Barker, P.A., Mackay, A.W., Ryves, D.B.*, et al.* (2016) An experiment to assess the effects of diatom dissolution on oxygen isotope ratios. *Rapid Commun. Mass Spectrom.* 30, 293-300. doi:10.1002/rcm.7446

Stolarski, J. (2003) Three-dimensional micro- and nanostructural characteristics of the scleractinian coral skeleton: A biocalcification proxy. *Acta Palaeontol Pol* 48, 497-530.

Straub, M. (2012) Application of foraminifera-bound nitrogen isotopes to Atlantic paleoceanography, Earth Science Department. ETH Zurich, Zurich.

Straub, M., Sigman, D.M., Auderset, A., Ollivier, J., Petit, B., Hinnenberg, B.*, et al.* (2021) Distinct nitrogen isotopic compositions of healthy and cancerous tissue in mice brain and head&neck micro-biopsies. *BMC Cancer* 21, 805. doi:10.1186/s12885-021-08489-x

Straub, M., Sigman, D.M., Ren, H., Martinez-Garcia, A., Meckler, A.N., Hain, M.P. and Haug, G.H. (2013) Changes in North Atlantic nitrogen fixation controlled by ocean circulation. *Nature* 501, 200-203. doi:10.1038/nature12397

Studer, A.S., Martinez-Garcia, A., Jaccard, S.L., Girault, F.E., Sigman, D.M. and Haug, G.H. (2012) Enhanced stratification and seasonality in the Subarctic Pacific upon Northern Hemisphere Glaciation-New evidence from diatom-bound nitrogen isotopes, alkenones and archaeal tetraethers. *Earth Planet. Sci. Lett.* 351, 84-94. doi:10.1016/j.epsl.2012.07.029

1203 Studer, A.S., Mekik, F., Ren, H., Hain, M.P., Oleynik, S., Martínez-García, A*., et al.* (2021) Ice
1204   Age-Holocene Similarity of Foraminifera-Bound Nitrogen Isotope Ratios in the Eastern
1205   Equatorial Pacific. *Paleoceanography and Paleoclimatology* 36.
1206   doi:10.1029/2020pa004063
1207 Studer, A.S., Sigman, D.M., Martinez-Garcia, A., Benz, V., Winckler, G., Kuhn, G*., et al.* (2015)
1208   Antarctic Zone nutrient conditions during the last two glacial cycles. *Paleoceanography* 30,
1209   845-862. doi:10.1002/2014PA002745
1210 Studer, A.S., Sigman, D.M., Martínez-García, A., Thöle, L.M., Michel, E., Jaccard, S.L*., et al.*
1211   (2018) Increased nutrient supply to the Southern Ocean during the Holocene and its
1212   implications for the pre-industrial atmospheric CO_2 rise. *Nat Geosci* 11, 756-760.
1213   doi:10.1038/s41561-018-0191-8
1214 Swart, K.A., Oleynik, S., Martínez-García, A., Haug, G.H. and Sigman, D.M. (2021) Correlation
1215   between the carbon isotopic composition of planktonic foraminifera-bound organic matter
1216   and surface water pCO_2 across the equatorial Pacific. *Geochim. Cosmochim. Acta* 306,
1217   281-303. doi:10.1016/j.gca.2021.03.007
1218 Tomiak, P.J., Penkman, K.E.H., Hendy, E.J., Demarchi, B., Murrells, S., Davis, S.A*., et al.*
1219   (2013) Testing the limitations of artificial protein degradation kinetics using known-age
1220   massive Porites coral skeletons. *Quat Geochronol* 16, 87-109.
1221   doi:10.1016/j.quageo.2012.07.001
1222 Van Cappellen, P., Dixit, S. and van Beusekom, J. (2002) Biogenic silica dissolution in the
1223   oceans: Reconciling experimental and field-based dissolution rates. *Global Biogeochemical*
1224   *Cycles* 16, 23-21-23-10. doi:10.1029/2001gb001431
1225 Van Eynde, E., Lenaerts, B., Tytgat, T., Verbruggen, S.W., Hauchecorne, B., Blust, R. and
1226   Lenaerts, S. (2014) Effect of pretreatment and temperature on the properties of Pinnularia
1227   biosilica frustules. *RSC Adv.* 4, 56200-56206. doi:10.1039/c4ra09305d
1228 Wang, X.C.T., Prokopenko, M.G., Sigman, D.M., Adkins, J.F., Robinson, L.F., Ren, H.J*., et al.*
1229   (2014) Isotopic composition of carbonate-bound organic nitrogen in deep-sea scleractinian
1230   corals: A new window into past biogeochemical change. *Earth Planet. Sci. Lett.* 400, 243-
1231   250. doi:10.1016/j.epsl.2014.05.048
1232 Wang, X.T., Sigman, D.M., Cohen, A.L., Sinclair, D.J., Sherrell, R.M., Cobb, K.M*., et al.* (2016)
1233   Influence of open ocean nitrogen supply on the skeletal delta N-15 of modern shallow-
1234   water scleractinian corals. *Earth Planet. Sci. Lett.* 441, 125-132.
1235   doi:10.1016/j.epsl.2016.02.032
1236 Wang, X.T., Sigman, D.M., Prokopenko, M.G., Adkins, J.F., Robinson, L.F., Hines, S.K*., et al.*
1237   (2017) Deep-sea coral evidence for lower Southern Ocean surface nitrate concentrations
1238   during the last ice age. *Proceedings of the National Academy of Sciences of the United*
1239   *States of America* 114, 3352-3357. doi:10.1073/pnas.1615718114
1240 Weigand, M.A., Foriel, J., Barnett, B., Oleynik, S. and Sigman, D.M. (2016) Updates to
1241   instrumentation and protocols for isotopic analysis of nitrate by the denitrifier method.
1242   *Rapid Commun. Mass Spectrom.* 30, 1365-1383. doi:10.1002/rcm.7570
1243 Weiner, S. and Erez, J. (1984) Organic matrix of the shell of the foraminifer, Heterostegina
1244   depressa. *The Journal of Foraminiferal Research* 14, 206-212. doi:10.2113/gsjfr.14.3.206
1245 Weiss, I.M., Muth, C., Drumm, R. and Kirchner, H.O.K. (2018) Thermal decomposition of the
1246   amino acids glycine, cysteine, aspartic acid, asparagine, glutamic acid, glutamine, arginine
1247   and histidine. *BMC Biophysics* 11. doi:10.1186/s13628-018-0042-4

1248   Whelan, J.K. (1977) Amino acids in a surface sediment core of the Atlantic abyssal plain.
1249   *Geochim. Cosmochim. Acta* 41, 803-810. doi:10.1016/0016-7037(77)90050-3
1250   Wolf, N., Carleton, S.A. and Martínez del Rio, C. (2009) Ten years of experimental animal
1251   isotopic ecology. *Functional Ecology* 23, 17-26. doi:10.1111/j.1365-2435.2009.01529.x
1252   Yoshioka, S. and Kitano, Y. (1985) Transformation of aragonite to calcite through heating.
1253   *Geochem J* 19, 245-249. doi:10.2343/geochemj.19.245
1254   Zheng, Y., Anderson, R.F., Froelich, P.N., Beck, W., McNichol, A.P. and Guilderson, T. (2002)
1255   Challenges in Radiocarbon Dating Organic Carbon in Opal-Rich Marine Sediments.
1256   *Radiocarbon* 44, 123-136. doi:10.1017/s0033822200064729
1257